IODP
INTERNATIONAL OCEAN DISCOVERY PROGRAM

International Ocean Discovery Program Expedition 395 Preliminary Report

Reykjanes Mantle Convection and Climate: Mantle Dynamics, Paleoceanography and Climate Evolution in the North Atlantic Ocean

12 June–12 August 2023

Ross Parnell-Turner, Anne Briais, Leah LeVay, and the Expedition 395 Scientists

Publisher's notes

Core samples and the wider set of data from the science program covered in this report are under moratorium and accessible only to Science Party members until 21 January 2025.

This publication was prepared by the *JOIDES Resolution* Science Operator (JRSO) at Texas A&M University (TAMU) as an account of work performed under the International Ocean Discovery Program (IODP). This material is based upon work supported by the JRSO, which is a major facility funded by the National Science Foundation Cooperative Agreement Number OCE1326927. Funding for IODP is provided by the following international partners:

National Science Foundation (NSF), United States
Ministry of Education, Culture, Sports, Science and Technology (MEXT), Japan
European Consortium for Ocean Research Drilling (ECORD)
Ministry of Science and Technology (MOST), People's Republic of China
Australia-New Zealand IODP Consortium (ANZIC)
Ministry of Earth Sciences (MoES), India

Portions of this work may have been published in whole or in part in other IODP documents or publications.

Disclaimer

Copyright

Citation

Parnell-Turner, R., Briais, A., LeVay, L., and the Expedition 395 Scientists, 2024. Expedition 395 Preliminary Report: Reykjanes Mantle Convection and Climate. International Ocean Discovery Program. https://doi.org/10.14379/iodp.pr.395.2024

ISSN

World Wide Web: 2372-9562

May 2024

Expedition 395 participants

Expedition 395 scientists

Ross E. Parnell-Turner
Co-Chief Scientist
Institute of Geophysics & Planetary Physics
Scripps Institution of Oceanography
University of California, San Diego
USA
rparnellturner@ucsd.edu

Anne Briais
Co-Chief Scientist
Geo-Ocean
Centre National de la Recherche Scientifique (CNRS)
Institut Universitaire Européen de la Mer
France
anne.briais@univ-brest.fr

Leah J. LeVay
Expedition Project Manager/Staff Scientist
International Ocean Discovery Program
Texas A&M University
USA
levay@iodp.tamu.edu

Ying Cui
Organic Geochemist
Department of Earth and Environmental Studies
Montclair State University
USA
cuiy@montclair.edu

Anita Di Chiara
Paleomagnetist
Istituto Nazionale di Geofisica e Vulcanologia
Italy
anita.dichiara@ingv.it

Justin P. Dodd
Inorganic Geochemist
Earth, Atmosphere and Environment
Northern Illinois University
USA
jdodd@niu.edu

Deepa P. Dwyer
Physical Properties Specialist
College of Earth Ocean and Atmospheric Sciences
Oregon State University
USA
shahde@oregonstate.edu

Deborah E. Eason
Petrologist
Department of Earth Sciences
University of Hawaii at Manoa
USA
deborahe@hawaii.edu

Sarah A. Friedman
Paleomagnetist
School of Earth, Environment & Sustainability
Georgia Southern University Statesboro Campus
USA
sfriedman@georgiasouthern.edu

Sidney R. Hemming
Physical Properties Specialist
Lamont-Doherty Earth Observatory
Columbia University
USA
sidney@ldeo.columbia.edu

Katharina E. Hochmuth
Downhole Tools/Physical Properties Specialist
Institute of Marine and Antarctic Studies (IMAS)
College of Science and Engineering
University of Tasmania
Australia
Katharina.Hochmuth@utas.edu.au

Halima Ibrahim
Sedimentologist
Department of Earth Sciences
Binghamton University
USA
hibrahi6@binghamton.edu

Claire Jasper
Sedimentologist
Lamont-Doherty Earth Observatory
Columbia University
USA
cjasper@ldeo.columbia.edu

Tom Dunkley Jones
Micropaleontologist (nannofossils)
School of Geography, Earth and Environmental Sciences
University of Birmingham
United Kingdom
t.dunkleyjones@bham.ac.uk

Boris T. Karatsolis
Micropaleontologist (nannofossils)
Department of Earth Sciences
Uppsala University
Sweden

Also at
Archaeology, Environmental Changes & Geo-Chemistry research group (AMGC)
Vrije Universiteit Brussel
Belgium
boris.karatsolis@vub.be

†Shore-based participant.

Saran Lee
Sedimentologist
Department of Natural Environmental Studies
The University of Tokyo
Japan
lee.saran.587@gmail.com

Danielle E. LeBlanc[†]
Sedimentologist
Department of Earth and Environmental Sciences
Boston College
USA
leblandf@bc.edu

Melody R. Lindsay
Inorganic Geochemist
Bigelow Laboratory for Ocean Sciences
USA
mlindsay@bigelow.org

David D. McNamara
Downhole Tools/Physical Properties Specialist
Department of Earth, Ocean and Ecological Sciences
University of Liverpool
United Kingdom
d.mcnamara@liverpool.ac.uk

Sevasti E. Modestou
Sedimentologist
Department of Geography and Environmental Sciences
Northumbria University
United Kingdom
sevi.modestou@northumbria.ac.uk

Bramley Murton[†]
Petrologist
Marine Geoscience Group
National Oceanography Centre
United Kingdom
bjm@noc.ac.uk

Suzanne B. O'Connell
Sedimentologist
Department of Earth and Environmental Sciences
Wesleyan University
USA
soconnell@wesleyan.edu

Gabriel T. Pasquet
Petrologist
Complex Fluids and Reservoirs Laboratory
University of Pau and Pays de l'Adour
France
gabriel.pasquet@univ-pau.fr

Paul N. Pearson
Micropaleontologist (planktonic foraminifers)
Department of Earth Sciences
University College London
United Kingdom
p.pearson@ucl.ac.uk

Sheng-Ping Qian[†]
Petrologist
School of Ocean and Earth Science
Tongji University
China
qianshengping@126.com

Yair Rosenthal[†]
Physical Properties Specialist/Stratigraphic Correlator
Institute of Marine and Coastal Sciences
Rutgers, The State University of New Jersey
USA
rosentha@marine.rutgers.edu

Sara Satolli[†]
Paleomagnetist
Department of Engineering and Geology
University of Chieti-Pescara
Italy
sara.satolli@unich.it

Matthias Sinnesael
Physical Properties Specialist/Stratigraphic Correlator
Institut de mécanique céleste et de calcul des éphémérides (IMCCE)
Observatoire de Paris
France
matthias.sinnesael@obspm.fr

Takuma Suzuki
Micropaleontologist (planktonic foraminifers)
Marine Core Research Institute
Kochi University
Japan
zaku142@gmail.com

Thena Thulasi Doss
Sedimentologist
Geosciences Division
National Centre for Polar and Ocean Research (NCPOR)
India
thenadoss@ncpor.res.in

Nicholas J. White
Physical Properties Specialist
Bullard Laboratories
Department of Earth Sciences
University of Cambridge
United Kingdom
njw10@cam.ac.uk

Tao Wu
Petrologist
Ocean College
Zhejiang University
China
taowu@zju.edu.cn

Alexandra Y. Yang[†]
Inorganic Geochemist
Guangzhou Institute of Geochemistry
Chinese Academy of Sciences
China
yangyang@gig.ac.cn

Outreach

Jennifer C. Field
Outreach Officer
Weston Massachusetts High School
USA
jcfield4@gmail.com

Operational and technical staff

Siem Offshore AS officials

Jake Robinson
Master of the Drilling Vessel

Mark Robinson
Drilling Supervisor

JRSO shipboard personnel and technical representatives

Alejandro Avila Santis
Marine Laboratory Specialist

Susan Boehm
Marine Laboratory Specialist

William Dan Cary
Applications Developer

Enrico De Pano
Marine Computer Specialist

David Fackler
Applications Developer

Fabricio Ferreira
Marine Laboratory Specialist

Clayton Furman
Schlumberger Engineer

Randy Gjesvold
Marine Computer Specialist

Kevin Grigar
Operations Superintendent

Mark Higley
Marine Laboratory Specialist

James Kowalski
Curatorial Specialist

Aidan Leetz
Marine Laboratory Specialist

Tiffany Liao
Marine Laboratory Specialist

Chang Liu
Marine Laboratory Specialist

Daniel Marone
Assistant Laboratory Officer

Aaron Mechler
Marine Laboratory Specialist

Beth Novak
Assistant Laboratory Officer

Chieh Peng
Laboratory Officer

Claudio Robustelli Test
Marine Laboratory Specialist/Imaging Specialist

Lars Daniel Rudback
Marine Laboratory Specialist

Alyssa Stephens
Publications Specialist

Steven Thomas
Marine Computer Specialist

Garrick Van Rensburg
Marine Computer Specialist

Abstract

The intersection between the Mid-Atlantic Ridge and Iceland hotspot provides a natural laboratory where the composition and dynamics of Earth's upper mantle can be observed. Plume-ridge interaction drives variations in the melting regime, which result in a range of crustal types, including a series of V-shaped ridges (VSRs) and V-shaped troughs (VSTs) located south of Iceland. Mantle upwelling beneath Iceland dynamically supports regional bathymetry and may lead to changes in the height of oceanic gateways, which in turn control the flow of deep water on geologic timescales. This expedition recovered basaltic samples from crust that is blanketed by thick sediments, that also contain climatic and oceanic records from modern to earliest Oligcene/late Eocene times. Major, trace, and isotope geochemistry of basalts from this expedition provide insight into spatial and temporal variations in mantle melting processes. These samples will enable testing of the hypothesis that the Iceland plume thermally pulses on two timescales (5–10 and ~30 Ma), leading to fundamental changes in crustal architecture. This idea will be tested against alternative hypotheses involving propagating rifts and buoyant mantle upwelling. Millennial-scale paleoclimate records are contained in the rapidly accumulated sediments of contourite drifts cored during Expedition 395. The accumulation rate of these sediments is a proxy for current strength, which is moderated by dynamic support of oceanic gateways such as the Greenland-Scotland Ridge. These sediments also provide constraints for climatic events including Miocene and Pliocene warmth, the intensification of Northern Hemisphere glaciation, and abrupt Late Pleistocene climate change. The integrated approach of Expedition 395 allows the relationships between deep Earth processes, ocean circulation, and climate to be explored. These objectives were addressed by recovering sediment and basement cores from four sites, plus an additional two sites which were completed during Expeditions 384 and 395C (U1555 and U1563). Two sites (U1554 and U1562) are located in Björn drift above a VSR/VST pair, and another site targeted the Holocene–Eocene sequence of sediments at Eirik drift, located on the eastern Greenland margin (U1602). The fourth site of Expedition 395 (U1564) is located on 32.4 My-old oceanic crust that is devoid of V-shaped features, and was chosen because it intersects the Holocene to Oligo–Miocene sedimentary sequence of Gardar drift. Considered together, the sediments, basalts and vast array of measurements collected during Expedition 395 will provide a major advance in our understanding of mantle dynamics and the linked nature of Earth's interior, oceans, and climate.

Plain language summary

In the North Atlantic Ocean, hot rocks are thought to rise up beneath Iceland from deep within Earth's interior, called the mantle, forming a giant mantle plume. This plume likely plays a key role in shaping the ocean crust around Iceland, including a pattern of distinctive crustal V-shaped ridges (highs) and V-shaped troughs (lows) that extend hundreds of kilometers on the seabed south of Iceland. Some think that these V-shaped ridges are generated by increases and decreases in plume activity, but their precise origin is hotly debated. Plume activity variations may also have contributed to changes in the height of oceanic gateways—passages that link Greenland, Iceland, and Scotland, thus controlling the amount of cold, deep water that has been flowing from the Norwegian Sea to the Atlantic Ocean over the past few million years. These deepwater currents deposit sediments on the seabed very quickly, recording the ambient ocean and climatic conditions along the way. As a result, the sediments contain a high-resolution record of the past, which we can measure in deep-sea cores. Expedition 395 cored through these sediments at four sites; at one of which, coring continued for 170 m into the ocean crust. Core, fluid, and microbial samples, along with measurements of the physical properties of both the core and the interior of the boreholes, will enable scientists to decipher processes taking place in the mantle, ocean, and climate over the past 32 million years.

1. Introduction

Scientific ocean drilling has transformed our understanding of Earth over the past five decades, from insights into past climates to the confirmation of plate tectonic theory. However, the con-

vecting behavior of Earth's mantle and its effects on surface processes such as ocean circulation and climate remains poorly understood. Basaltic rocks erupted at mid-ocean ridges (MORs) provide a window into mantle processes. When MORs are located near large upwellings called mantle plumes, interactions between these two systems produce variations in mantle composition and dynamics that are recorded at the ridges. Although mantle plumes (e.g., beneath Hawaii) are fairly common, intersecting plume-ridge systems are unusual. One such intersecting system is located in the North Atlantic Ocean, where the Iceland mantle plume is strongly influenced by the Mid-Atlantic Ridge, which includes the Reykjanes Ridge southwest of Iceland. Basaltic rocks erupted at the spreading axis record the geochemical signature of the underlying mantle and the melting and extrusion processes, providing a record of the composition and dynamics of the mantle plume and its interaction with the spreading system. The Reykjanes Ridge flanks host a series of V-shaped crustal ridges and troughs, whose origin has been long debated. One of the hypotheses to explain the formation of these ridges is that the Iceland mantle plume has been pulsing at a frequency of several millions of years, causing melt anomalies and driving transient uplift of the surrounding North Atlantic region on geological timescales. Other hypotheses to explain these ridges do not require pulsing of the Iceland plume.

Basins around the Reykjanes Ridge are blanketed by rapidly accumulating sediments that record the oceanographic conditions on thousand-year timescales, providing some of the most detailed climate records on Earth (Figure **F1**). Southward-flowing deepwater currents in the North Atlantic Ocean deposit fine-grained sediments called contourite drifts, which accumulate at rates of hundreds of meters per million years. The Reykjanes Ridge flanks are the site of major contourite drift deposits. Two of these, the Björn and Gardar drifts, are located on the eastern flank of the ridge. In contrast, Eirik drift consists of an elongate, mounded contourite deposit that is plastered along the East Greenland margin. Vertical motions caused by variations in the Iceland mantle plume temperature could have altered the depth of the oceanic gateways connecting the Norwegian and Greenland Seas into the North Atlantic Ocean, with implications for deepwater circulation, sediment deposition, and climate. In addition, over time, basaltic crust spreads away from the ridge, and interact with the overlying seawater and sediments, becoming progressively altered because of hydrothermal circulation and chemical exchange. The unique juxtaposition of a mantle plume, a spreading ridge, oceanic gateways, and rapidly accumulating sediment provide an ideal natural laboratory to test multidisciplinary ideas about the interactions between Earth's deep and surficial domains. Although the rich scientific potential in this region was demonstrated during Deep Sea Drilling Project (DSDP) Leg 49 and Ocean Drilling Program (ODP) Leg 162 (Luyendyk

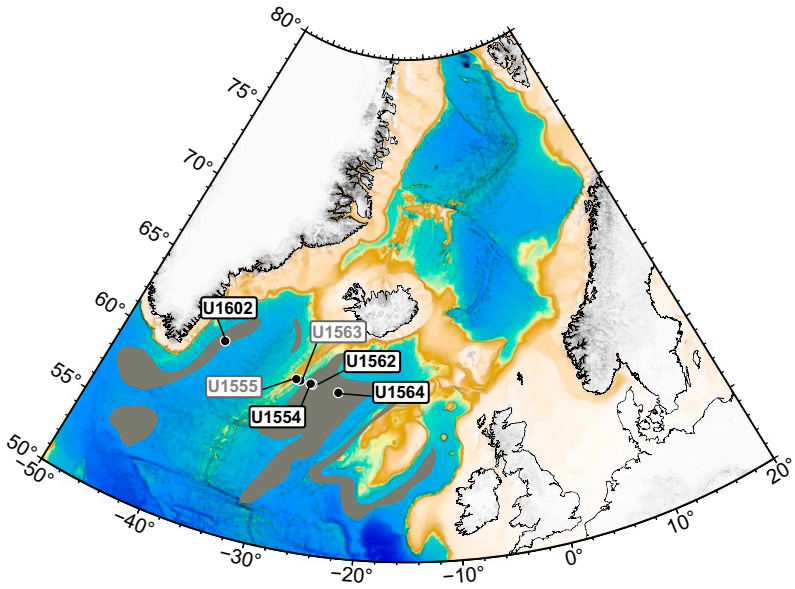

Figure F1. Bathymetry of North Atlantic Ocean. Black labels = Expedition 395 sites, gray labels = Expedition 384 and 395C sites, brown polygons = contourite drifts.

et al., 1979; Jansen and Raymo, 1996), comprehensive sampling of both the sediment and underlying basaltic crust is still lacking. A transect of holes has been drilled during Expeditions 384, 395C and 395 to address three major objectives: (1) to test the control of the time-dependent behavior of the Iceland mantle plume on crustal accretion at the Reykjanes Ridge; (2) to obtain high-resolution records of climate and ocean circulation near major North Atlantic oceanic gateways; and (3) to track the accretion, aging, and hydrothermal exchange of oceanic crust over 32 My.

2. Background

2.1. Geologic setting

As new basaltic oceanic crust is formed, it draws material from the underlying mantle, so rocks recovered from MORs have long been used to measure the thermal and compositional properties of the mantle (e.g., Krause and Schilling, 1969; Hart et al., 1973; Schilling, 1973). Where MORs lie above mantle plumes, such as along Reykjanes and Kolbeinsey Ridges near Iceland, oceanic crustal accretion is thought to be influenced by plume activity (e.g., White, 1997). Close agreement between models of dynamic topography and seismic tomography supports the idea that mantle upwelling beneath Iceland influences the entire North Atlantic region today (Hartley et al., 2011; Rickers et al., 2013; Schoonman et al., 2017). A possible sign of time-dependent plume behavior is the set of diachronous V-shaped ridges (VSRs) and V-shaped troughs (VSTs) that straddle the Reykjanes Ridge south of Iceland (Figure **F2**). Vogt (1971) first suggested that the VSRs reflect variations in crustal thickness caused by pulses of hotter asthenosphere advecting horizontally away from the Iceland plume that episodically increase the thickness of crust formed at the axis.

Oceanic crustal accretion is sensitive to small mantle potential temperature perturbations, which can change the thickness of newly formed material by hundreds of meters to kilometers (White et al., 1995). The ratios between incompatible trace elements, such as Nb/Y, are largely insensitive to crustal processes such as fractional crystallization, and reflect the depth and degree of melting. A southward decrease of Nb/Y on the Reykjanes Ridge correlates with deepening of the axis, with a decrease in crustal thickness but also with decreasing source enrichment estimated by isotopic indicators such as $^{87}Sr/^{86}Sr$ (Murton et al., 2002; Shorttle and Maclennan, 2011). Variations in incompatible trace element ratios can be observed along axis, which correlate with patterns in gravity anomaly, bathymetry and earthquake seismicity (Parnell-Turner et al., 2013; Jones et al., 2014). Compositional variations associated with VSRs cannot be explained by fractional crystallization alone because a corresponding variation in Mg number is absent. Because enrichment in

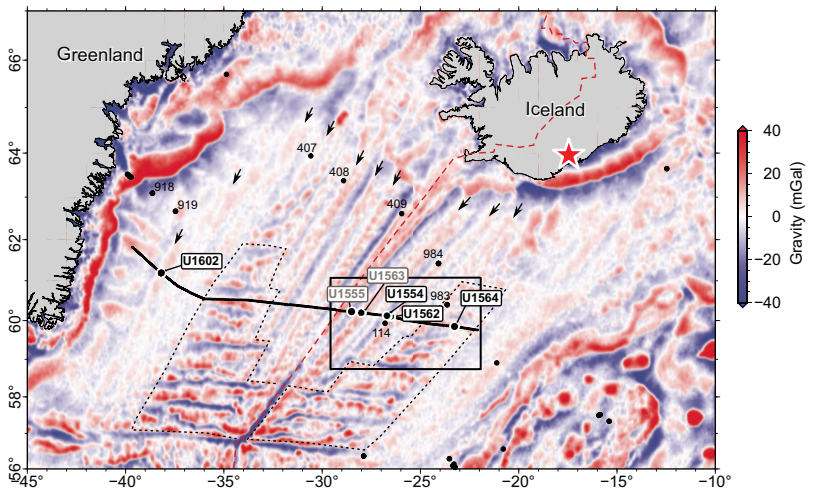

Figure F2. Free-air gravity anomaly filtered to remove wavelengths > 250 km. Solid black line = Seismic Profile JC50-1, black labels along seismic profile = Expedition 395 sites, gray labels = Expedition 384 and 395C sites, small black circles = DSDP/ODP sites, dashed red line = Mid-Atlantic Ridge, red star = Iceland plume center (Shorttle and Maclennan, 2011), arrows = VSRs, dotted polygons = transition from smooth to segmented ocean floor, black box = location of Figure F4.

incompatible trace elements is inversely correlated with crustal thickness, mantle temperature variation is thought to play an important role in controlling crustal thickness, in addition to changes in mantle source fusibility (Poore et al., 2011; Parnell-Turner et al., 2017).

Since Vogt's early thermal pulsing hypothesis, the origin of the VSRs has been debated (Figure **F3**) (e.g., Parnell-Turner et al., 2014). One alternative idea is that the VSRs may be tectonic in origin and have no requirement for melt anomalies originating from temperature variations in the mantle plume itself (Briais and Rabinowicz, 2002; Rabinowicz and Briais, 2002; Benediktsdóttir et al., 2012). In this hypothesis, a sequence of propagating rifts and southward migrating discontinuities, suggested by the observed asymmetric accretion at the ridge axis, explains the formation of VSRs and VSTs, which are thought to represent ridge segments and pseudofault scarps, respectively (Figure **F3**). A third hypothesis, in which shallow buoyant mantle upwelling instabilities propagate along axis to form the observed crustal structure variations, has also been suggested; it avoids the requirement for rapid mantle plume flow (Figure **F3**) (Martinez and Hey, 2017; Martinez et al., 2019).

Crust on the Reykjanes Ridge was last drilled in 1978, during DSDP Leg 49 when basalts were recovered at three sites (Sites 407, 408 and 409), all located on VSRs. A total basalt thickness of 453 m was penetrated (Luyendyk et al., 1979), leading to a series of breakthroughs in our understanding of the nature and scale of mantle heterogeneity and crustal accretion under the influence of a mantle plume (e.g., Wood et al., 1979; Dupré and Allègre, 1980; Fitton et al., 1997). The deepest basement penetration was at Site 409 located 23 km from the ridge axis, where 240 m of vesicular basalt was drilled in the 2.4 My old crust; however, the other Leg 49 sites are on older crust (36 and 20 Ma) and did not attempt to recover basalts from a VST. Hence, Leg 49 basalts alone are not able to unravel the origins of VSRs and VSTs, and do not provide detailed step-wise information about the aging of oceanic crust.

The North Atlantic Ocean is separated from the colder, more dense waters of the Arctic Ocean and Norwegian-Greenland Sea by the Greenland-Scotland Ridge (GSR), which represents a critical gateway affecting Cenozoic deepwater circulation patterns and climate. The GSR is generally less than 500 meters below sea level (mbsl) and is only ~1000 mbsl at its deepest point, making the overflow flux sensitive to small variations in the ridge depth. Reconstructions of Neogene mantle plume activity correlate with deepwater circulation patterns in the North Atlantic (Wright and

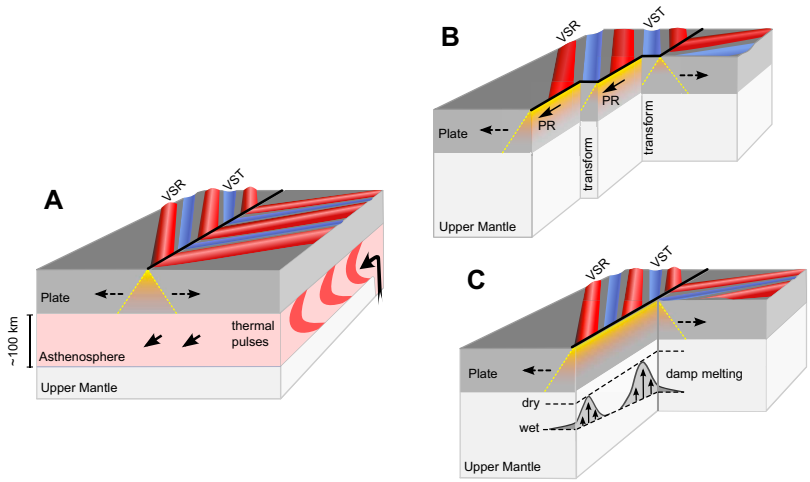

Figure F3. Competing hypotheses for VSR formation (Parnell-Turner et al., 2017). A. Thermal pulsing hypothesis (Vogt, 1971). Dark gray blocks = lithospheric plates, pink block with red patches = asthenospheric channel containing thermal pulses, light gray block = upper mantle, solid arrows = propagation direction of thermal pulses, dashed arrows = plate spreading direction, yellow shading = melting region, red/blue ribs = VSRs/VSTs, black line = MOR. B. Propagating rift hypothesis (Hey et al., 2010). Solid arrows = propagating rift direction. VSRs are regarded as failed rifts with thicker crust and VSTs are regarded as pseudofaults that propagate along axis generating thinner crust. C. Buoyant mantle upwelling hypothesis (Martinez and Hey, 2017). Gray blobs = buoyant upwelling cells that generate damp melting and thicker crust in absence of thermal anomaly, vertical arrows = vertical upwelling in a given cell, dashed lines = dry/wet solidi.

Miller, 1996). Inferred times of high mantle plume activity are linked to low Northern Component Water productivity, increased current strength, and sedimentary deposition rates (Wright and Miller, 1996; Poore et al., 2006; Parnell-Turner et al., 2015). Southward-flowing deepwater currents in the North Atlantic Ocean deposit fine-grained sediments called contourite drifts, which accumulate at rates of hundreds of meters per million years. Two contourite drifts, Gardar and Björn, were successfully drilled during Leg 162 (Jansen and Raymo, 1996), providing a record of drift sedimentation back to early Pleistocene and late Pliocene times (~2 and 3 Ma). High sedimentation rate combined with near 100% core recovery rates means that these sites contain some of the highest resolution records of ocean circulation and climate to date (Kleiven et al., 2011; Thornalley et al., 2013). These records can be directly compared to atmospheric records from ice cores and provide a unique, high-resolution insight into the Earth's climatic past (Barker et al., 2019).

2.2. Site survey data

A detailed geophysical survey of Reykjanes Ridge and its flanks was conducted in June–July 2010 during RRS *James Cook* Cruise JC50, collecting more than ~2400 km of 2D multichannel reflection seismic data (Parnell-Turner et al., 2015, 2017). The survey consisted of two basin-spanning regional seismic reflection profiles, oriented parallel to plate-spreading flowlines, and a series of 19 shorter perpendicular crossing lines. These multichannel data are of sufficient quality to identify the sediment/basement interface, as well as potential drilling hazards such as faults, gas accumulations, and stratigraphic discontinuities. Primary and alternate sites were positioned on thick sediment or in localized sedimentary basins that were imaged on seismic reflection profiles so that holes could easily be established. Sites were chosen as close to crossing seismic profiles as possible while avoiding sedimentary disturbances, faults, and basement discontinuities. Sediment thicknesses are estimated using interval sediment velocities from ODP Leg 162 where possible, and stacking velocities are used for deeper levels.

3. Scientific objectives

3.1. Objective 1: crustal accretion and mantle plume behavior

Expedition 395 aimed to use the composition of basaltic samples to understand crustal formation south of Iceland at two temporal scales. First, on ~5–10 My timescales, we sought to test three alternative hypotheses for the formation of VSRs: (1) thermal pulsing, (2) propagating rifts, and (3) buoyant mantle upwelling. Drilling allowed us to test these hypotheses, which predict differing depths, temperatures, and degrees of melting between VSRs and VSTs recorded in basalt composition. Dredged samples are restricted to the ridge axis because deep-sea corals and sediments cover off-axis areas (Murton et al., 2002; Jones et al., 2014). Hence, off-axis VSRs and VSTs can only be sampled by drilling. Second, we aimed to test the controls on crustal architecture over longer, ~30–40 My timescales. Oceanic crust south of Iceland can be divided into two distinct structural types—smooth and segmented—using gravity, magnetic and bathymetric data sets (e.g., White, 1997). Smooth oceanic crust contains VSRs and VSTs but also exhibits seafloor magnetic anomalies that are largely unbroken by fracture zone offsets, similar to those more typical at fast-spreading ridges. Segmented oceanic crust exhibits traces of ridge axis discontinuities that are more typical of slow-spreading ridges; hence, the seafloor here represents a microcosm of global variability in crustal structure. The location of the boundary between smooth and segmented crustal styles has shifted through time (Jones et al., 2002). This transition has been proposed to reflect changes in melt supply to the ridge and may record expansion and contraction of the Iceland plume over ~35 My. Segmented oceanic crust usually forms above cooler asthenosphere or at slow-spreading ridges, whereas smooth crust usually forms above relatively hot asthenosphere close to plume heads or at intermediate- to fast-spreading ridges. Therefore, in the North Atlantic Ocean, small changes in melt flux, temperature, and/or spreading behavior may drive regime changes in crustal architecture. Our objective of understanding how crustal formation responds to mantle temperature, degree of melting, and plume activity can be achieved by comparing the geochemistry of basalts from smooth and segmented crustal domains.

3.1.1. Basalt geochemistry

The accretion of oceanic crust is sensitive to small mantle potential temperature perturbations, which can change the thickness of newly formed material by hundreds of meters to kilometers (White et al., 1995). Basalt trace element ratios, such as Nb/Y, can be largely insensitive to crustal processes such as fractional crystallization and reflects the depth and degree of melting. A southward decrease of Nb/Y between 63°N and 61°N on Reykjanes Ridge correlates with deepening of the axis, a decrease in crustal thickness, and decreasing source enrichment estimated by isotopic indicators such as $^{87}Sr/^{86}Sr$ and $^{143}Nd/^{144}Nd$ (Murton et al., 2002; Jones et al., 2014).

Leg 49 yielded major advances in understanding of mantle heterogeneity (e.g., Wood et al., 1979), plume structure (e.g., Fitton et al., 1997), and melting processes (e.g., Kempton et al., 2000). However, the location of these sites precludes their use to address the temporal and spatial variability of plume dynamics. Expedition 395 sites, located along a spreading-parallel flowline, avoid the issue of variable distance from the plume. Incompatible trace element concentrations and ratios (e.g., Nb/Y and La/Sm) will be used to constrain melting models, building upon previous work on the axis. Major and trace element concentrations will be used to constrain differences in the composition, depth, and extent of melting between VSR/VST pairs and segmented crust unaffected by VSRs. Indirect reconstruction of axial depth is possible using volatile elements such as carbon, water, and sulfur, which de-gas when erupted at the seafloor. For example, advances in understanding the CO_2 concentration in ridge basalts enable quantification of eruption pressure (Le Voyer et al., 2017). Recovery of basaltic glass during Expedition 395 will enable electron and ion-probe analyses to measure volatile elements and therefore estimate eruption pressures and test the plume pulsing hypothesis.

Objective 1 of the Expedition 395 project addresses 2050 Science Framework Strategic Objective 2: Ocean Life Cycle of Tectonic Plates, which concerns the formation, aging and eventual destruction of oceanic plates. The coincidence of Reykjanes Ridge with the Iceland plume provides an opportunity to observe the composition and behavior of Earth's interior, as recorded by oceanic crust. Major, rare earth, and trace element concentrations of basalts recovered from Expedition 395 sites will be used to constrain mantle melting models to investigate how crust forms on slow-spreading ridges.

Crustal architecture south of Iceland is dominated by two main features: the diachronous VSRs that straddle Reykjanes Ridge and the transition from smooth to segmented oceanic crust that took place at ~35 Ma. These features may have been formed because of the interaction between time-dependent mantle convection and plate spreading or a series of propagating rifts or patches of buoyant mantle upwelling. By using similar basalt geochemistry and isotopic systematics, we will investigate changes in mantle temperature and composition that coincide with the changes in spreading style (Figure **F4**). In addition, the transect of sites are situated on crust of progressively increasing age and varying sedimentary cover. Basalts from Expedition 395 sites exhibit varying degrees of alteration along the transect, recording the progressive aging of the oceanic crust as it interacts with seawater, sediment, and possibly microbial life over millions of years, as explained below as part of Objective 3.

3.2. Objective 2: oceanic circulation, gateways, and sedimentation

Cores and data from Expedition 395 sites allow us to quantify how oceanic circulation in the North Atlantic Ocean has varied since Oligocene times. Deep water flow in the North Atlantic is dominated by two oceanic gateways, the Iceland-Faroe Ridge and the Denmark Strait, that control the southward flow of water from the Norwegian Sea and exert a major influence on global ocean circulation (Figure **F5**).

The rate of accumulation of contourite drift sediments in the North Atlantic Ocean is primarily controlled by deepwater flow along bathymetric rises; hence, the strength and pathways of deep-water currents are recorded by these drift sediments (e.g., Wright and Miller, 1996). These deposits provide an indirect proxy for temporal variations in deep water flow. Additionally, short-term climatic effects relating to the location of oceanic fronts during both glacial–interglacial and (shorter) stadial–interstadial cycles may play a role in circulation patterns on shorter timescales

(thousands of years). It has been suggested that uplift and subsidence of the Iceland-Faroe Ridge and Denmark Strait are influenced by mantle upwelling beneath Iceland and that there may therefore be an indirect connection between ocean circulation and mantle plume behavior (e.g., Parnell-Turner et al., 2015; Poore et al., 2011). Age-depth relationships at the six Expedition 395 sites will allow us to test the proposed correlation between mantle plume activity and ocean circulation by using sediment accumulation rates as a first-order proxy for deep water current strength. The oldest previously drilled sediments in the Iceland Basin are ~3 Ma (Jansen and Raymo, 1996), and Expedition 395 extends that record back to ~32 Ma, allowing us to investigate the relationships between mantle convection, oceanic gateway configuration, and climate.

High sedimentation rates of contourite drift deposits in the North Atlantic Ocean (12–16 cm/ky) have led to paleomagnetic and isotopic records that are among the most detailed available (Channell et al., 2002). Existing boreholes provide high-resolution climate records back to 1.7 Ma (Site 983), and this program extends the high-resolution climate record further into late Pliocene times. Coring the full depth of Gardar drift at Site U1564, Björn drift at Sites U1554 and U1562, and into pre-drift Oligocene–Miocene sediments provides long-term constraints on sedimentation rates and the potential for climate reconstructions across long timescales. Work on Leg 162 sites demonstrates the utility of sediments for millennial-scale reconstructions of surface and deep-

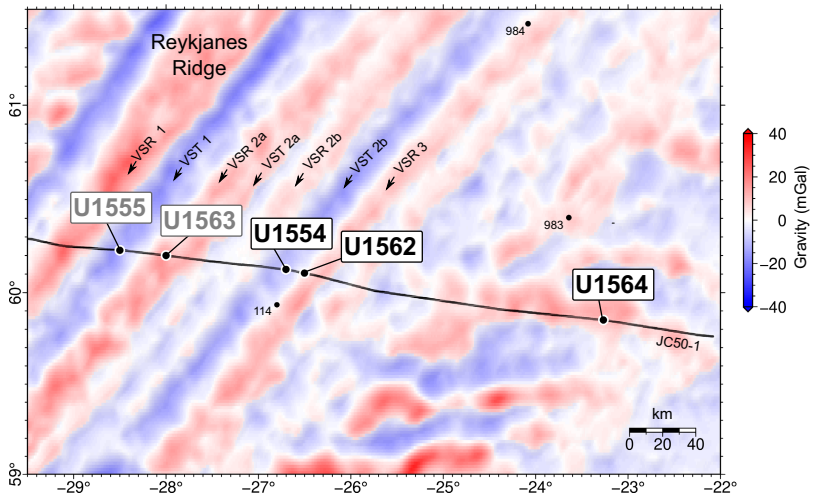

Figure F4. Free-air gravity anomaly filtered to remove wavelengths > 250 km. Solid black line = Seismic Profile JC50-1, black labels along seismic profile = Expedition 395 sites, gray labels = Expedition 384 and 395C sites, small black circles = ODP sites.

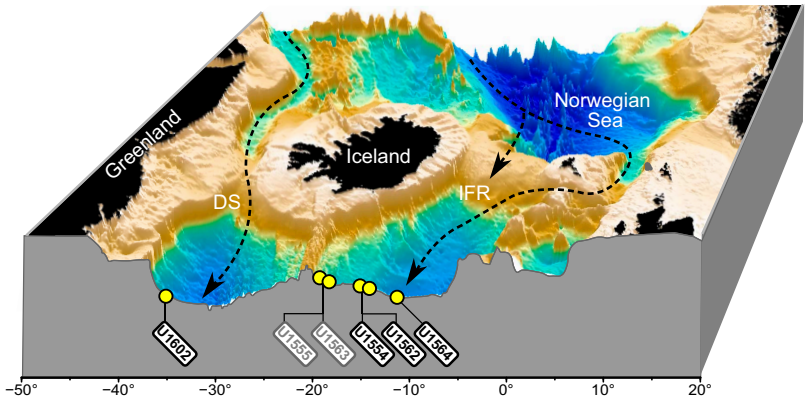

Figure F5. Three-dimensional perspective view, Expedition 395 sites. Yellow circles with black labels = Expedition 395 sites, yellow circles with gray labels = Expedition 384 and 395C sites, dotted lines = overflow of deep water from Norwegian Sea, via Denmark Strait (DS) and Iceland-Faroe Ridge (IFR).

water properties (Barker et al., 2015, 2019; Raymo et al., 1998). Planktonic foraminifer counts give a first-order constraint on sea-surface temperatures and the latitudinal migration of the polar front, which fluctuates in line with millennial-scale temperature recorded by Greenland ice cores over the past ~100 ky (Bond et al., 1993). Similar relationships can be derived for intervals beyond the reach of Greenland ice cores, documented by the similarity between climate and %*Neogloboquadrina pachyderma* (e.g., ODP Site 983). Ice-rafted debris (IRD) is a useful tracer for rafted ice, which can be associated with cold/freshening surface conditions that are proposed to affect ocean circulation through changes in surface buoyancy (Menviel et al., 2014). Intensive ice rafting has occurred in the North Atlantic since northern hemisphere glaciation onset at around 2.7 Ma (Bailey et al., 2013), and its occurrence at Site 983 has been used to document millennial-scale variability over the past 1.2 My. Sediments on the Björn and Gardar drifts experienced changes in accumulation rate due to variations in deepwater overflow of proto-North Atlantic Deep Water. Variations in the vigor of these overflows are detected using the sortable silt proxy (McCave et al., 2017); this approach has been used at Sites 983 and 984 to track overflow changes on submillennial timescales (Kleiven et al., 2011; Thornalley et al., 2013). These proxies, in combination with foraminifer oxygen isotopes (for temperature/salinity) and carbon (deep ocean mixing) give the potential to reconstruct submillennial variations in ocean properties throughout the interval of drift deposition.

Expedition 395 addresses 2050 Scientific Framework Strategic Objective 3: Earth's Climate System and Strategic Objective 4: Feedbacks in the Earth System. Subsidence and uplift of the Denmark Strait and Iceland-Faroe Ridge may have controlled the deepwater exchange between the Arctic Ocean, Nordic Seas, and Atlantic Ocean. Under this hypothesis, the tectonic evolution of these oceanic gateways and sills modifies large-scale ocean circulation, which is a component of multiple climate feedback loops. Thus, the histories of these gateways and their associated deepwater flow are central to our understanding of Northern Hemisphere climate and its interaction with global thermohaline circulation. Sediments at Expedition 395 drilling sites were accumulated at high rates and therefore provide a millennial-scale paleoclimate record since drift initiation. This extended record spans the critical middle Pliocene intervals when global mean surface temperatures were 2°–3°C warmer than today. We will be able to test the sensitivity of ocean circulation to changes in gateway conditions, which will inform boundary conditions for climate models targeting key future analogue warm climate states, such as the mid-Pliocene. Finally, the record of crustal alteration across the five crustal sites will enable us to examine the styles and process of crustal weathering that likely plays a role in modulating CO_2 sequestration on long timescales.

3.3. Objective 3: time-dependent hydrothermal alteration of oceanic crust

Sites cored during Expedition 395 address the nature, extent, timing and duration of hydrothermal alteration of oceanic crust formed at the Reykjanes Ridge. Hydrothermal circulation along MORs and across their flanks is responsible for one-third of the heat loss through the ocean crust (Sclater et al., 1980; Bodine et al., 1981). It influences tectonic, magmatic, and microbial processes on a global scale and is a fundamental component of global biogeochemical cycles (Coggon and Teagle, 2011). There is also growing evidence that the long-term carbon cycle is influenced by the reaction of seawater with the oceanic crust in low-temperature, off-axis hydrothermal systems, perhaps representing an important mechanism for carbon drawdown (e.g., Gillis and Coogan, 2011). The relative contribution of this process remains controversial because we do not know how much low-temperature alteration takes place off axis. Although the nature of individual hydrothermal fluid-rock reactions is generally understood, the magnitude and distribution of chemical exchange remain poorly quantified, as does the partitioning between high- and low-temperature exchange with crustal age. Consequently, the role of the production, hydrothermal alteration, and subsequent subduction of ocean crust in key global geochemical cycles remains uncertain. Drilled sections of hydrothermally altered crust from the Reykjanes Ridge flank provide time-integrated records of geochemical exchange between crust and seawater along an age transect from 2.8 to 32.4 Ma (Figure **F6**). The recovered cores, fluid samples, and wireline logging data will enable us to quantify the timing and extent of hydrothermal fluid–rock exchange across the Reykjanes Ridge

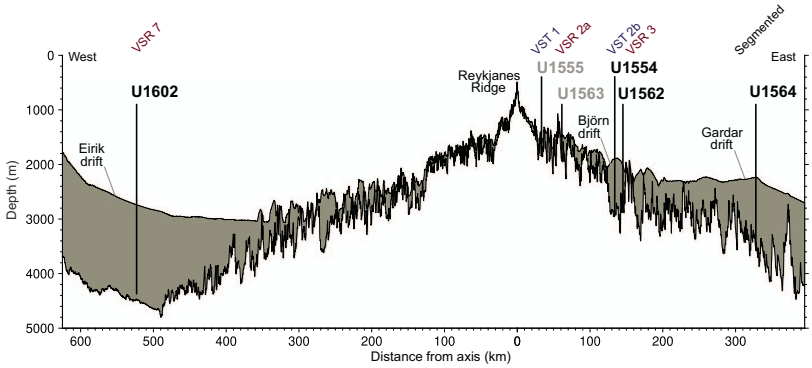

Figure F6. Depth transect showing seafloor depth, sediment/basement interface depth, sedimentary thickness (shading), and Expedition 395 sites (gray labels = Expedition 384 and 395C sites). Figure based on Seismic Profile JC50-1 and velocity model from Parnell-Turner et al. (2017).

flank and to assess the hydrothermal contributions of a rapidly sedimented slow-spreading ridge flank to global geochemical budgets.

The ocean-basin–wide transect drilled during Expedition 395 spans crust from 2.8 to 32 My in age, which has experienced a spectrum of different sedimentation, geochemical, and hydrogeologic processes. Expedition 395 project Sites U1555, U1563, U1554, U1562 and U1564 comprise a west-to-east crustal flow line transect across the eastern flank of Reykjanes Ridge. The recovered cores sample the uppermost ~130–200 m of lavas produced 2.8, 5.2, 12.4, 14.2, and 32.4 My ago at the Reykjanes Ridge, which provide a unique opportunity to quantify the timing and extent of hydrothermal fluid–rock exchange in a slow-spreading ridge flank that experienced rapid sedimentation and variations in tectonic architecture. These sites address 2050 Science Framework Strategic Objective 2: Oceanic Life Cycle of Tectonic Plates.

Expedition 395 project sites provide an exceptionally large variety of subseafloor environments in which to study microbial communities, aiding in the understanding of the habitability of life on Earth, 2050 Science Framework Strategic Objective 1. The comprehensive set of samples collected for microbiological analyses in cores from shallow to deep sedimentary sequences, sediment/basement interface, and from deep within the basement will provide insights into the factors controlling the development of life. These analyses will benefit from the comprehensive record of the corresponding geochemical environment provided by the interstitial fluid, sediment, basement rocks and their alteration products collected at all sites.

4. Site summaries

4.1. Site U1554

4.1.1. Background and objectives

Expedition 395 Site U1554 (proposed Site REYK-6A) is located in the North Atlantic Ocean along the Reykjanes Ridge south of Iceland and on Björn drift (Figure **F1**). Site U1554 is located on Seismic Line JC50-1 (common midpoint [CMP] 41740), near the intersection with line JC50-C3 (CMP 1005), both obtained in 2010 during RRS *James Cook* Cruise JC50. Site U1554 is located in VST 2b with an estimated basement age of 12.7 Ma. Another target for Site U1554 is to obtain a continuous sedimentary record of the Björn drift, which is expected to offer millennial-scale climate records. The sedimentation rate of this drift can serve as a proxy for deep water current strength and provide information for testing proposed on vertical oceanic gateway motions and their potential ties to pulsing behavior of the Iceland mantle plume.

Cores and data from this site will address all three of the primary science objectives of Expedition 395: (1) crustal accretion and mantle behavior; (2) ocean circulation, gateways, and sedimentation; and (3) time-dependent hydrothermal alteration of oceanic crust.

4.1.2. Operations

Site U1554 (proposed Site REYK-6A) (60°07.5060′N, 26°42.0960′W) consists of 8 holes drilled during Expeditions 384, 395C, and 395 (Table T1). Holes U1554A–U1554D were cored during Expedition 384 in July 2020. These holes range 23.5–76.0 m drilling depth below seafloor (DSF). The recovered cores were used to create a stratigraphic splice of the section. Holes U1554E and U1554F were cored and logged during Expedition 395C in 2021. These holes extended to 647.7 and 779.9 m DSF, respectively. Finally, Holes U1554G and U1554H were each cored to ~355 m DSF during Expedition 395.

The sediments and basalts recovered on Expeditions 384 and 395C were sampled for select shipboard measurements during the cruises. Cores from these two expeditions were described postcruise at a core description party held at the Gulf Coast Repository in College Station, Texas, USA in May 2022.

A total of 194 cores were recovered for Site U1554. Over a 1683.9 m cored interval, these cores collected 1611.82 m of sediment and basalt (96%).

The total time spent at Holes U1554A to U1554F was 21.78 days: 2.02 days during Expedition 384, 16.26 days during Expedition 395C, and 3.5 days during Expedition 395.

Below we summarize operations and scientific results from all three expeditions.

Table T1. Hole summary, Expedition 395. * = reentry system installed.

Hole	Latitude	Longitude	Water depth (mbsl)	Total penetration (mbsf)	Drilled interval (m)	Cored interval (m)	Recovered length (m)	Recovery (%)	Cores (*N*)	APC cores (*N*)	HLAPC cores (*N*)	XCB cores (*N*)	RCB cores (*N*)
U1554G	60°7.5037′N	26°42.1129′W	1868.7	355.0	0.0	355.0	362.29	102	40	31	3	6	0
U1554H	60°7.4952′N	26°42.1188′W	1866.7	354.9	0.0	354.9	370.10	104	38	30	0	8	0
		Site U1554 totals:		709.9	0.0	709.9	732.40	103	78	61	3	14	0
U1562C	60°6.3015′N	26°30.0754′W	2002.8	300.4	7.0	293.4	308.45	105	48	15	33	0	0
		Site U1562 totals:		300.4	7.0	293.4	308.45	105	48	15	33	0	0
U1564D	59°51.0483′N	23°16.0080′W	2208.1	657.3	2.0	655.3	632.42	97	73	22	6	45	0
U1564E	59°51.0485′N	23°15.9876′W	2207.3	263.5	0.0	263.5	273.70	104	28	22	0	6	0
U1564F	59°51.0363′N	23°15.9840′W	2208.1*	1169.7	598.0	571.7	434.15	76	75	0	0	0	75
		Site U1564 totals:		2090.5	600.0	1490.5	1340.30	99	176	44	6	51	75
U1602A	61°11.7138′N	38°10.8186′W	2708.6	8.8	0.0	8.8	8.81	100	1	1	0	0	0
U1602B	61°11.7144′N	38°10.8184′W	2709.2	251.1	0.0	251.1	262.37	104	38	16	22	0	0
U1602C	61°11.7253′N	38°10.8193′W	2710.0	269.3	2.0	267.3	272.63	102	38	19	19	0	0
U1602D	61°11.7259′N	38°10.7967′W	2709.1	540.7	0.0	540.7	450.45	83	66	19	18	29	0
U1602E	61°11.7150′N	38°10.7961′W	2709.2	1365.2	529.3	835.9	450.39	54	87	0	0	0	87
		Site U1602 totals:		2435.1	531.3	1903.8	1444.70	76	230	55	59	29	87
		Expedition 395 totals:		5535.9	1138.3	4397.6	3825.80	84	532	175	101	94	162

Hole	Date started (2023)	Time started UTC (h)	Date finished (2023)	Time finished UTC (h)	Time on hole (days)	Time on site (days)
U1554G	27 Jun	1845	29 Jun	1745	1.96	
U1554H	29 Jun	1745	1 Jul	0645	1.54	
				Site U1554 totals:		3.50
U1562C	1 Jul	1215	3 Jul	0900	1.86	
				Site U1562 totals:		1.86
U1564D	21 Jun	1500	25 Jun	2015	4.22	
U1564E	25 Jun	2015	27 Jun	0640	1.43	
U1564F	25 Jul	2100	10 Aug	2200	16.04	
				Site U1564 totals:		21.69
U1602A	4 Jul	1718	5 Jul	0500	0.49	
U1602B	5 Jul	0500	6 Jul	1600	1.46	
U1602C	6 Jul	1600	8 Jul	0530	1.56	
U1602D	8 Jul	0530	11 Jul	1645	3.47	
U1602E	11 Jul	1645	24 Jul	0409	12.48	
				Site U1602 totals:		19.46
				Expedition 395 totals:		46.51

4.1.2.1. Expedition 384

4.1.2.1.1. Hole U1554A

The vessel arrived at Site U1554 at 0600 h on 27 July 2020. The thrusters were lowered and the ship switched to dynamic positioning (DP) mode at 0629 h, ending the 1100 nmi transit from Kristiansand, Norway. An advanced piston corer (APC)/extended core barrel (XCB) bottom-hole assembly (BHA) was made up and deployed at 1445 h. Hole U1554A (60°07.5038′N, 26°42.0955′W; 1869.7 mbsl) was spudded at 2300 h. Cores 1H–8H were advanced to 72.2 m DSF. Following Core 8H, the pipe was pulled up and the bit cleared the seafloor at 0625 on 28 July, ending Hole U1554A. A total of 8 APC cores with 74.71 m of core were recovered from a 72.2 m interval (104% recovery).

4.1.2.1.2. Hole U1554B

The vessel was offset 20 m east of Hole U1554A, and Hole U1554B (60°07.5058′N, 26°42.0748′W; 1871.0 mbsl) was spudded at 0735 h on 28 July 2020. Cores 1H–8H recovered 76.77 m of core over the 76.0 m cored interval (101%). Hole U1554B ended at 1500 h on 28 July when the bit cleared the seafloor.

4.1.2.1.3. Hole U1554C

The ship was offset 20 m south of Hole U1554B. Hole U1554C (60°07.4950′N, 26°42.0747′W; 1869.0 mbsl) was spudded at 1600 h on 28 July 2020. Cores 1H–8H were collected over a 75.0 m interval with 77.03 m of core recovered (103%). The drill pipe was pulled from the hole and the bit cleared the seafloor at 2345 h on 28 July, ending Hole U1554C.

4.1.2.1.4. Hole U1554D

The vessel was offset 20 m west of Hole U1554C. Hole U1554D (60°07.4941′N, 26°42.0968′W; 1869.0 mbsl) was spudded at 0055 h on 29 July 2020. The hole was washed down to 14 m DSF and Core 2H was collected from 14.0 to 23.5 m DSF, and 9.72 m of sediment was recovered (102%). This core was collected for the future testing of the shipboard track systems and was not curated or included as part of the Expedition 395/395C project.

Following coring operations, the drill pipe was pulled out of the hole with the bit clearing the seafloor at 0140 h and the rotary table at 0715 h on 29 July. The drill string and BHA were broken down and the vessel was secured for transit at 0820 h. The thrusters were raised and the ship began the transit to Site U1555 at 0900 h on 29 July, ending operations at Site U1554 during Expedition 384.

4.1.2.2. Expedition 395C

4.1.2.2.1. Hole U1554E

Following a 54 nmi transit from Site U1555, the vessel arrived at Site U1554 early on 24 June 2021. At 0754 h, Hole U1554E (60°7.5235′N, 26°42.1324′W; 1869.8 mbsl) was spudded using the APC/XCB system and drilled without recovery to 66.3 m DSF. Coring using the APC system progressed from 66.3–218.3 m DSF (Cores 2H–17H) with 157.92 m of sediment recovered (104%). Cores 18X–62X (218.3–647.7 m DSF) were collected with 383.15 m of core recovered (89%). The basement was encountered at ~647 m DSF while drilling Core 62X; the core contained 1 m of basalt interlayered with carbonate sediment. The final hole depth was 647.7 m DSF. A total of 61 cores were collected at Hole U1554E, with 541.07 m of core collected over a 581.4 m interval (93%).

The drill string was pulled up to 72.8 m DSF for downhole logging. Two runs each with the triple combination (triple combo) and Formation MicroScanner (FMS)-sonic tool strings were completed for the length of the borehole. Following logging operations, the drill string was pulled out of the hole with the bit clearing the seafloor at 2210 h on 28 June. At 0245 h on 29 June the bit cleared the rotary table, ending the hole.

4.1.2.2.2. Hole U1554F

The ship was positioned over the Hole U1554F coordinates (60°7.5136′N, 26°42.1140′W; 1869.7 mbsl), ~25 m southeast of Hole U1554E, and the rig floor crew began assembling the casing and reentry system. The casing and drill string were run to 1552 mbsl and the subsea camera system

was deployed to observe the casing operations. Hole U1554F was spudded at 1345 h, and the casing was drilled into the hole to 602 m DSF. The drill string was pulled from the hole with the bit clearing the seafloor at 1610 h on 1 July 2021.

The drill string was assembled with a rotary core barrel (RCB) BHA and Hole U1554F was reentered at 1057 h on 2 July. The drill string advanced to the base of the casing. Hole U1554F was then drilled without recovery to 620 m DSF. Two drilled intervals were recorded for the hole. Cores 3R–5R advanced from 620 to 649.1 m DSF, and 19.86 m of core was recovered (68%). Core 5R contained the sediment/basement interface at ~647 m DSF. Cores 6R–20R advanced from 649.1 to 721.7 m DSF, and 45.91 m of basalt was recovered (63%).

Following recovery of Core 395C-U1554F-20R, the drill string was pulled from the hole to change the drill bit. The bit cleared the seafloor at 1840 h and rotary table at 2210 h on 5 July 2021. The drill string reentered Hole U1554F at 0405 h on 6 July. RCB coring resumed from 721.7–779.9 m DSF with the recovery of Cores 21R–32R.

In total, 30 cores over an interval of 159.9 m were recovered from Hole U1554F. The core recovery for this hole was 100.15 m (63%). The basement cores were advanced at an average rate of 1.76 m/h.

Following coring operations, the hole was conditioned for downhole wireline logging. The drill pipe was pulled out of the hole and the subsea camera deployed to observe operations. The drill bit cleared the seafloor at 0643 h on 8 July and the ship was offset 20 m to the northeast. The bit was released at 0756 h and at 0955 h the pipe reentered Hole U1554F. The drill string was deployed to 589.2 m DSF inside the casing string. The triple combo logging tool string was made up and run for two passes of the borehole from the base of the casing string (602 m DSF), to the bottom of the hole at 779 m DSF. At 2010 h, the triple combo tool string reached the drill floor and was broken down. The FMS-sonic tool string was made up and run at 0410 h on 9 July and completed two passes of the borehole. The Ultrasonic Borehole Imager (UBI) tool string was then made up and deployed to the bottom of the hole with two logging passes. The drill pipe was pulled up from 588 m DSF to 69 m DSF in preparation of running the Versatile Seismic Imager (VSI) from the base of the hole up through the casing string. However, foggy conditions throughout the afternoon and evening inhibited visibility and prevented the start of the protected species observation (PSO) protocols. At daybreak, visibility had worsened and conditions were not forecast to improve until evening. Because of the time already allocated to Site U1554, the decision was made to abandon the VSI logging run and begin operations at Site U1562. The drill pipe was pulled up and cleared the seafloor at 0755 h on 10 July, ending Hole U1554F.

The vessel returned to Hole U1554F on 21 July 2021 to attempt to complete the VSI logging operations. The ship completed the 6.1 nmi transit in DP mode from Site U1562 to Hole U1554F at 0730 h. The drill string reentered Hole U1554F at 0930 h and the pipe was run to 68.5 m DSF in the casing string to prepare for downhole logging with the VSI tool. Fog had formed around the vessel and after waiting until 1250 h, the VSI was deployed to the base of the casing string. Nearly immediately whales were spotted in the exclusion zone, which delayed the start of the VSI operations. After 2 h of tracking whales in the vicinity of the vessel, foggy conditions reduced visibility prohibiting the continuation of PSO watch. With the fog forecast to worsen throughout the evening and into the next day, the planned VSI operations were canceled at 1600 h in favor of coring at the next site. The drill pipe was pulled out of the hole and the end of the pipe cleared the seafloor at 1840 h and the rig floor at 2210 h on 21 July. The rig floor was secured for transit and the thrusters were raised. The vessel began the 39 nmi transit to Site U1563 at 2236 h, ending operations at Hole U1554F and Site U1554 during Expedition 395C.

4.1.2.3. Expedition 395

4.1.2.3.1. Hole U1554G

Following a 104 nmi transit from Site U1564, the ship arrived at Site U1554 at 1800 h on 27 June 2023. The thrusters were lowered, and the vessel switched to DP mode, beginning Hole U1554G (60°7.5037′N, 26°42.1129′W; 1868.7 mbsl) at 1842 h. Hole U1554G was spudded at 0340 h on 28 June and recovered 5.43 m of sediment. Cores 1H–31H were advanced to 288.4 m DSF. After

reaching refusal of the APC system, the half-length APC (HLAPC) was deployed for Cores 32F–34F (288.4–302.5 m DSF).

XCB coring advanced the hole from 302.5 to 355.0 m DSF, recovering Cores 395-U1554G-35X through 40X. The target depth of the hole was achieved, and the drill string was pulled out of the hole with the bit clearing the seafloor at 1745 h on 29 June, marking the end of Hole U1554G. A total of 40 cores were taken in Hole U1554G over the 355.0 m cored interval. Core recovery was 102% and 362.3 m of sediment was collected.

4.1.2.3.2. Hole U1554H

The ship was offset 20 m south of Hole U1554G. At 2135 h on 29 June 2023, Hole U1554H (60°07.49852′N, 26°42.1188′W; 1866.7 mbsl) was spudded with Core 1H, and 9.4 m was recovered. Cores 1H–30H advanced to 280.1 m DSF.

The decision was made to switch to the XCB system when the overpull on the core barrels increased and Cores 395-U1554H-31X through 38X (280.1–354.9 m DSF) were collected. After reaching the target depth, the drill string was pulled out of the hole. The drill bit cleared the seafloor at 0640 h on 1 July, ending Hole U1554H and operations at Site U1564. The vessel began the transit in DP mode to Site U1562. A total of 38 cores were recorded for Hole U1554H, with 370.1 m of core recovered across a 354.9 m interval (104%).

4.1.3. Principal results

4.1.3.1. Sedimentology

The Holocene to middle Miocene sediments cored at Site U1554 are relatively homogeneous, primarily composed of silty clay with varying but minor amounts of siliceous and carbonate microfossils, as well as minor proportions of sand (Figure **F7**). Near the sediment/basement interface, the sediments transition to nannofossil chalk. Core recovery through the sedimentary sequence is near-continuous in the upper 475 m. Based on the observations of sediment composition along with the attenuation pattern of natural gamma radiation (NGR), magnetic susceptibility (MS), and calcium carbonate ($CaCO_3$) weight percent, Site U1554 is divided into four lithostratigraphic Units (I–IV). Units I, II, and IV include two subunits. The measured $CaCO_3$ varies from 0.26 to 84.76 wt%. Features of note include glass layers, bands of variable color at unit or subunit boundaries, basaltic and metamorphic clasts, shell fragments, and halo/pyritized and silt-filled burrows.

4.1.3.2. Igneous petrology

The cores from Hole 395C-U1554F are dominated by slightly to moderately altered basalt (Figure **F7**). An additional meter of basalt was also recovered in Hole 395C-U1554E. The contact between the basalt and overlying sedimentary strata was partly recovered across Cores 395C-U1554F-4R through 6R. In Hole 395C-U1554F, detailed core observations reveal a series of sheet flows and pillow lavas. The sheet flows consist of hypocrystalline aphyric olivine basalt. Flow boundaries and fractures generally show brown alteration halos, especially in the upper third of the hole, and vesicles are often filled. The pillow lavas are highly fragmented with glass rinds, chilled margins, and vesicle bands. In the upper 40 m of the basement, thin sedimentary and volcanoclastic horizons are common, consisting of calcareous mudstone conglomerate layers and peperites. The peperites become increasingly baked and crystalline downhole. Thin section examination reveals fine-grained aphyric or sparsely olivine phyric basalts with low to moderate alteration. They contain abundant olivine microphenocrysts, as well as some large olivine phenocrysts with occasional spinel inclusions. The groundmass contains acicular and skeletal swallowtail plagioclase laths, rare clinopyroxene microcrystals, opaque oxides, and altered glass. The inferred volcanic stratigraphy consists of a sequence of interbedded extrusive sheet flows and pillow lavas with minor evidence of sediment deposition.

4.1.3.3. Alteration petrology

Basalt at Site U1554 (Holes 395C-U1554E and U1554F) predominantly contains background-type alteration, although localized alteration in the form of halos around fractures is present to a lesser degree. The alteration assemblage is chlorite+Fe-oxide/oxyhydroxides+clay with minor carbonate. In thin section, saponite and chlorite dominate the alteration assemblage and disseminated magnetite is observed. Vesicles are commonly filled with celadonite, and to a lesser extent chlorite, Fe-

oxide/oxyhydroxides, carbonate, zeolite, and rare sulfides. Basalt fragments in peperite intervals are variably altered to palagonite material.

Fracture density at Site U1554 is ~28 fractures per meter and is uniform with depth. Fracture mineral fill is dominantly Fe-oxide/oxyhydroxide+carbonate±chlorite with occasional clay and celadonite. Some fractures are filled with carbonate sediment in intervals where interlayered sediment and peperites are common. Alteration halos are observed around some fractures with colors including gray, brown, and brown with a gray border.

4.1.3.4. Micropaleontology

At Site U1554, a 647 m interval of upper Miocene to upper Pleistocene silty clay and nannofossil chalk was recovered across multiple holes. Micropaleontological analyses were undertaken on sediment samples to 647.7 m core depth below seafloor, Method A (CSF-A), in Hole 395C-U1554E

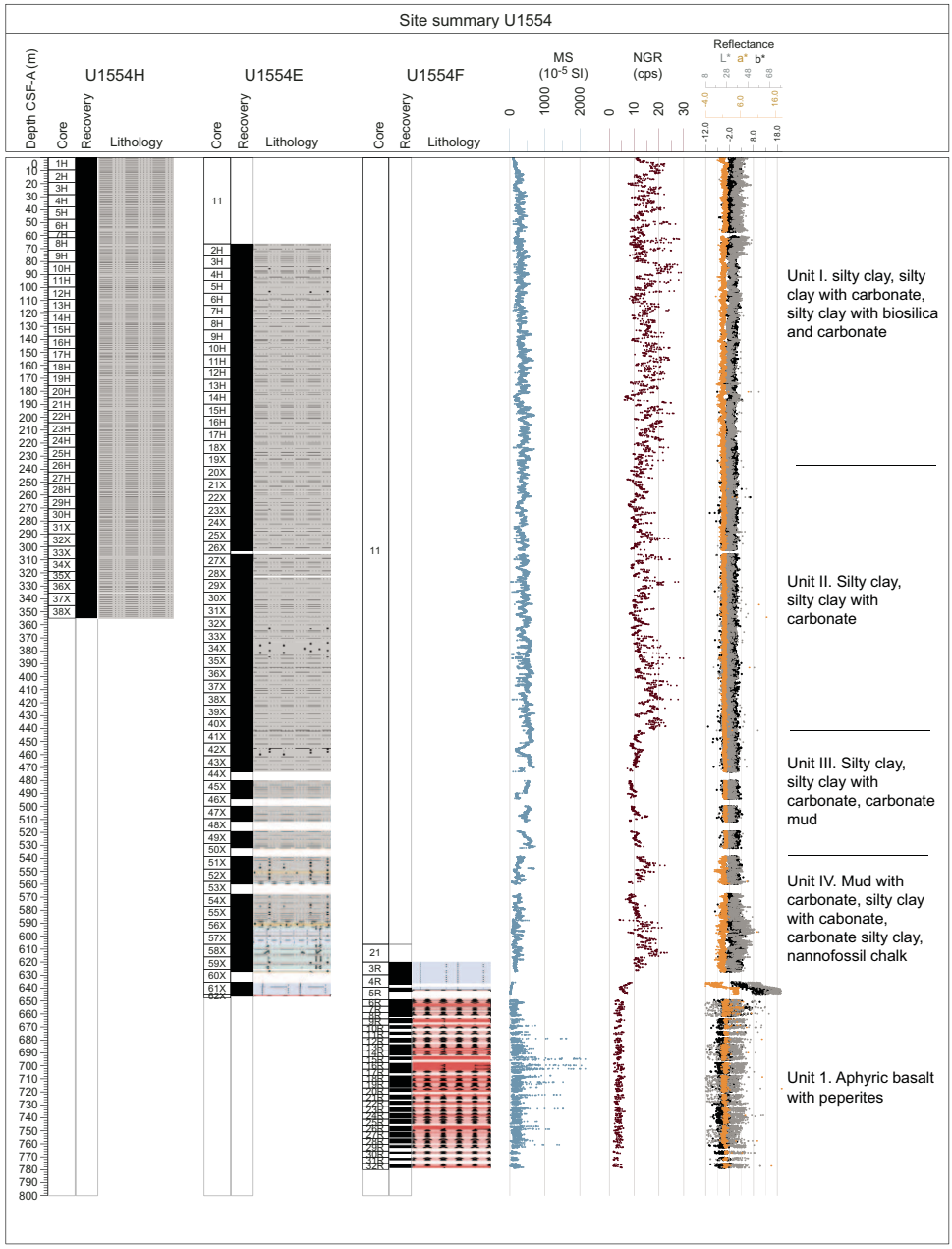

Figure F7. Lithostratigraphic summary, Site U1554. cps = counts per second, Roman numerals = sedimentary units, Arabic numerals = igneous units.

and to 354.97 m CSF-A in Hole 395-U1554G. Biohorizons used in the age model are based on calcareous nannoplankton, planktonic foraminifers, and bolboforms. Calcareous nannofossils and planktonic foraminifers are present with varying abundances, from barren or nearly barren samples to those with very high abundances. Bolboforms, when present, are always rare or few.

A total of eleven calcareous nannofossil Pleistocene biohorizons are identified in the upper 234.96 m CSF-A of Hole U1554G, representing ages of 0.09 to 1.71 Ma. Four nannofossil biohorizons are identified through the upper Miocene to Pliocene, including the biohorizon Top *Coccolithus miopelagicus*, which constrains the bottom of the hole to be older than 11.04 Ma. A total of five Pleistocene, two Pliocene, and three Miocene planktonic foraminifer biohorizons where recognized, with an estimated age of the base of the sediment section to be between 10.54 and 11.76 Ma. Four upper Miocene bolboform biohorizons are recognised with calibrated ages between 5.60 and 10.20 Ma. In the interval ~530 to 630 m CSF-A, glauconite is abundant in foraminifer sample residues.

4.1.3.5. Physical properties

At Site U1554, bulk density shows an increase from 1.4 to ~1.8 g/cm^3 from seafloor to 450 m CSF-A with noticeable increases and decreases superimposed on this trend. Both MS and NGR suggest similar oscillatory behavior to that observed in the bulk density. These variations become more pronounced below ~450 m CSF-A. Poor core recovery in Hole 395C-U1554E between 470–570 m CSF-A causes more detailed interpretations for physical properties to be challenging in this interval. The bottom ~80 m of Hole U1554E (570–647 m CSF-A) is characterized by variations in bulk density, a trend also expressed by the MS, color records, and more variable lithology. The limestone in the bottom two cores (395C-U1554E-61X and 62X) shows higher bulk densities (>1.8 g/cm^3), lower MS, lower NGR, and lighter colors compared to the overlaying sediments.

4.1.3.6. Stratigraphic correlation

A ~0–70 m splice for Holes U1554A–U1554C was previously constructed during Expedition 384. In the full splice, the upper 80 m core composite depth below seafloor (CCSF) interval is very similar to that produced during Expedition 384, and includes Holes U1554A–U1554C. From Core 395C-U1554E-2H, tied to Core 384-U1554A-7H from the initial splice, through Core 395-U1554H-23H, a continuous splice was constructed using only Holes 395C-U1554E and 395-U1554H. Between 225 and 345 m CCSF several gaps are unavoidable.

4.1.3.7. Paleomagnetism

Natural remanent magnetization (NRM) was measured for sedimentary cores recovered from Expedition 384 Holes U1554A–U1554C, Expedition 395C Holes U1554E and U1554F, and Expedition 395 Holes U1554G–U1554H. The cores were demagnetized with a stepwise alternating field cleaning protocol, with the exceptions of Hole U1554G and the upper part of Hole U1554H. The resolution of these measurements varies from 1 to 5 cm. The demagnetization step at 20 mT from Hole U1554E was used to establish an age-depth trend for the upper 400 m CSF-A in Site U1554. Between 400 m CSF-A and the bottom of Core 395C-U1554E-61X at 645 m CSF-A, apparent gaps in sediment deposition hampered interpretation of the magnetostratigraphy.

NRM was measured for basalt cores recovered in Hole 395C-U1554F. The basalts in Hole U1554F do not fully demagnetize at 25 mT but the drilling overprint is removed. The demagnetization reveals mostly normal polarities and one of two behaviors: (1) 80% magnetization loss before 25 mT or (2) no significant loss of magnetization by 25 mT. The variations in MS coincide with those in NRM intensity before and after demagnetization at 25 mT.

4.1.3.8. Geochemistry

Cores taken during Expeditions 384 (Hole U1554A), 395C (Holes U1554E and U1554F), and 395 (Holes U1554G and U1554H) were analyzed for headspace gas, interstitial water (IW) chemistry, and bulk sediment geochemistry. Headspace gas analyses were conducted at Holes U1554A and U1554E; methane concentrations are variable and range ~0–12,000 ppmv (Figure **F8**). Ethane was absent in all holes. Holes U1554E and U1554G were analyzed for IW chemistry and bulk sediment geochemistry. Calcium ion (Ca^{2+}) and magnesium ion (Mg^{2+}) concentrations display similar trends with depth. Sulfate ion (SO_4^{2-}) concentrations display a bimodal distribution with seawater-like

values at the top and bottom of the sediment column. $CaCO_3$ weight percent generally decreases downhole, trending from ~30 wt% at the top to ~17 wt% near the sediment/basement interface. Bulk sediment generally has low total organic carbon (TOC), total nitrogen (TN), and total sulfur (TS) content. Dissolved oxygen measurements were conducted on whole-round cores from Hole U1554G to ~347 m CSF-A (Core 40X).

4.1.3.9. Downhole logging

Logging operations were undertaken in Holes 395C-U1554E (~0–640 m wireline log depth below seafloor [WSF]) and 395C-U1554F (~604–770 m WSF). Hole U1554E was logged with the triple combo and FMS-sonic tool strings, and Hole U1554F was logged with the triple combo, FMS-sonic, and UBI tool strings. Logging responses at Site U1554 define five logging units, with subunits in Logging Units 1, 2, and 4. Logging Subunit 1a (0–75 m WSF) is defined by gamma log measurements collected through drill pipe, and Logging Subunit 1b (75–108 m WSF) is characterized by low density and low gamma log. Logging Unit 2 (108–440 m WSF) is characterized by cyclic, 1 to 10 m long fluctuations in gamma log, the peaks of which are dominated by high thorium counts. MS data shows a similar cyclic pattern in this logging unit. The cyclic gamma and MS logging responses occur at shorter wavelengths in Logging Subunit 2a (108–375 m WSF) than in Logging Subunit 2b (375–440 m WSF). Logging Unit 3 (440–495 m WSF) is marked by relatively lower gamma log and longer wavelength fluctuations in MS, and the density (~1.8 g/cm^3) and porosity (~0.6) in this unit are remarkably invariant. Logging Unit 4 (495–647 m WSF) is marked by relatively high gamma log and can be divided into three subunits: Logging Subunit 4a (495–535 m WSF) shows invariant V_P and V_S values, Logging Subunit 4b (535–635 m WSF) shows relatively high V_P and V_S (up to ≤ 2615 m/s and 850 m/s, respectively), and Logging Subunit 4c (635–647 m WSF) contains the lowermost sediment and the top of the sediment–basement transition zone, the top of which is marked by an abrupt decrease in density and increase in porosity. FMS borehole images for the sedimentary section of Site U1554 show decimeter-scale, shallow dipping, alternating conductive and resistive layers. Logging Unit 5 denotes the basaltic basement of Site U1554, with an increase in resistivity and density. The FMS and UBI borehole images show clear layering in the basalt basement, some of which contain numerous features that may represent fractures and basaltic pillow margins.

4.1.3.10. Age model

Age model tie points at Site U1554 are based upon paleomagnetic and paleontologic constraints. From the seafloor to the base of Matuyama Chron at 402.34 m CSF-A, the age model is based on magnetostratigraphic reversals complemented by calcareous nannofossil and planktonic foraminifer biostratigraphy. Below that level, a succession of magnetic polarity reversals is recorded, but their magnetostratigraphic interpretation is highly uncertain because of gaps in the record, so the age model relies on biostratigraphy alone, which is based on calcareous nannofossils, planktonic

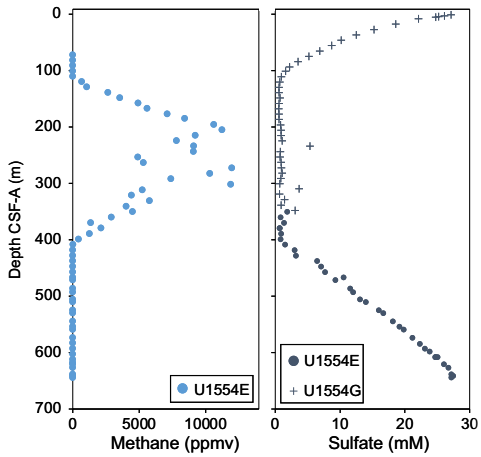

Figure F8. Composite gas analyses of methane concentrations and sulfate concentrations, Site U1554.

foraminifers, and bolboforms. The age at sediment/basement interface is extrapolated at ~12.15 Ma.

4.2. Site U1562

4.2.1. Background and objectives

Site U1562 (proposed Site REYK-3B) is located in the North Atlantic Ocean, east of the Reykjanes Ridge and on Björn contourite drift south of Iceland (Figure **F1**). Site U1562 is located on Seismic Line JC50-1 (CMP 39920), near the intersection with line JC50-C2 (CMP 685), both obtained in 2010 during RRS *James Cook* Cruise JC50.

Site U1562 is located on VSR 3, and has an estimated basement age of 13.86 Ma. The sediment section at Site U1562 is marked by the Björn drift deposit, a thicker section of which was cored at Site U1554.

Cores and data from this site will address all three primary science objectives: (1) crustal accretion and mantle behavior, (2) ocean circulation, gateways and sedimentation, and (3) time-dependent hydrothermal alteration of oceanic crust.

4.2.2. Operations

Site U1562 (60°06.3006′N, 26°30.1044′W) consisted of three holes, Holes 395C-U1562A, 395C-U1562B, and 395-U1562C, which range 300.4–561.5 m DSF (Table **T1**). A total of 144 cores were recovered for Site U1562. These cores collected 792.57 m of sediment and basalt over a cored interval of 876.5 m (90% recovery). Downhole wireline logging operations using four logging tools took place at Hole U1562B. The total time spent at Site U1562 was 12.3 days.

4.2.2.1. Expedition 395C

4.2.2.1.1. Hole U1562A

The vessel began the 6.1 nmi transit from Hole 395C-U1554F to Site U1562 under DP mode on 10 July 2021. At 1306 h on 10 July, the vessel arrived at Site U1562 and the APC/XCB BHA was made up.

Hole 395C-U1562A (60°06.3030′N, 26°30.1245′W; 2003 mbsl), located 21 m west of the site coordinates, was spudded at 2115 h on 10 July. Cores 1H–21H advanced from 0 to 192.0 m DSF. The HLAPC core barrels were made up and coring continued with Cores 22F–57F (192.0–361.2 m DSF) with 4.7 m advances. The XCB was deployed and cut Cores 58X–64X (361.2–429.1 m DSF). After recovering Core 64X, the XCB cutting shoe was severely damaged and slightly melted and the base of the core catcher contained basalt. Another core barrel was deployed and Core 65X was advanced to ensure that the bit had reached basement. The bit advanced 0.7 m over an hour and Core 65X contained 0.68 m of basalt (97% recovery), confirming a basement depth of 429.1 m DSF. The final depth of Hole U1562A was 429.8 m DSF. The drill string was pulled from the hole, with the bit reaching the seafloor at 1535 h on 13 July. Hole U1562A ended when the bit reached the rotary table at 1935 h.

4.2.2.1.2. Hole U1562B

Following the end of Hole 395C-U1562A, an RCB BHA with a C-4 RCB bit was made up and the drill string lowered to the seafloor. The ship was offset 21 m ESE of Hole U1562A, near the site coordinates, and Hole U1562B (60°6.2993′N, 26°30.1026′W; water depth 2003 mbsl) was spudded at 0320 h on 14 July 2021 and advanced without coring to 408.1 m DSF. The center bit was recovered and an RCB core barrel was deployed. Cores 2R–19R advanced from 408.1 to 500.7 m DSF. The sediment/basement interface was recovered in Core 4R at 429.0 m DSF. While coring Core 19R, the penetration rate dropped to 1 m/h and there was erratic torque on the bit. It was suspected that the drill bit was damaged and the rig floor crew began pulling the pipe out of the hole. A free-fall funnel was deployed at 0220 h on 17 July to allow for the reentry of Hole U1562B. The bit cleared the seafloor at 0312 h and the rotary table at 0708 h. The bit was indeed damaged and a new C-7 RCB coring bit was made up to the BHA and the crew assembled the drill string. The subsea camera, along with the Conductivity-Temperature-Depth (CTD) tool, was deployed at 1130 h to observe the reentry of Hole U1562B, which occurred at 1450 h. The subsea camera was

retrieved and the drill string advanced to 500.7 m DSF. After cleaning the hole with a high-viscosity mud sweep, Cores 20R–28R advanced from 500.7 to 561.5 m DSF. Coring operations concluded at Hole U1562B after coring 132.5 m into the basement section. The final depth of Hole U1562B was 561.5 m DSF.

Following coring, the rotary shifting tool was run to release the bit into the bottom of the hole. The drill string was pulled up and end of the pipe was set at 89 m DSF. The triple combo logging tool string was made up and deployed at 1755 h on 19 July. After completing two successful passes of the entire hole, the tools were retrieved and reached the rig floor at 2310 h. The FMS-sonic tool was made up and deployed at 0100 h on 20 July. Following two passes that extended to the base of the hole, the FMS-Sonic tool was pulled from the hole and reached the rig floor at 0645 h. The VSI was lowered to the base of the hole and a total of four depth stations (420.5, 426, 459.9, and 556.6 m DSF) were completed, two in the basement section, one at the sediment/basement interface, and one in the lowermost sediment. The final logging run, using the UBI, began at 1445 h. The UBI made two passes of the basement section, acquiring 360° borehole images. The UBI was recovered at the rig floor at 2130 h. The drill string was pulled out of the hole to ~1489 mbsl and the ship began the transit in DP mode to Hole 395C-U1554F at 2355 h on 20 July, ending Site U1562.

4.2.2.2. Expedition 395

4.2.2.2.1. Hole U1562C

The vessel returned to Site U1562 on 1 July 2023. Following a 6.1 nmi transit from Hole 395-U1554H, the vessel was over the site coordinates at 1210 h, marking the start of Hole 395-U1562C (60°06.3015′N, 26°30.0754′W; 2002.7 mbsl), which was spudded at 1500 h. Cores 1H–16H advanced the hole to 139.3 m DSF. Refusal of the APC system was reached at 139.3 m DSF and the HLAPC was deployed for the remainder of the hole. Cores 17F–53F advanced the hole to 300.4 m DSF. Five short, drilled intervals (1.5–2 m long) were used to offset coring gaps between Holes 395C-U1562A and 395-U1562C for stratigraphic correlation. After reaching the target depth of 300 m DSF, the drill pipe was pulled from the hole with the bit clearing the seafloor at 0405 h on 3 July. A total of 48 cores were collected at Hole U1562C, recovering 308.45 m of sediment over a 293.4 m cored interval (105% recovery). The BHA was broken down and the rig secured for transit. At 0900 h the ship was switched from DP to cruise mode, ending operations at Site U1562.

4.2.3. Principal results

4.2.3.1. Sedimentology

The sediments at this site include silty clay with variable amounts of carbonate (Lithostratigraphic Units I–III) and nannofossil chalk (Unit IV) (Figure **F9**). Based on smear slide observations, carbonate microfossils are present in amounts ranging from a few to over 30%. Siliceous microfossils are present throughout but in minor amounts (<10%). The terrigenous component is dominated by quartz and feldspar, although glauconite and glass are also present. Glass abundance increases from Unit I to Unit II. Immediately below the lithologic boundary between Units I and II there are several sharp contacts. Unit III is defined by the abundance of features consistent with soft sediment deformation, likely caused by a series of slumps. There is a sharp contact between Units III and IV. Weight percent $CaCO_3$ is variable, but average values increase downhole until the chalk in Unit IV. Small clasts of volcaniclastic material (pumice and scoria) and larger clasts of variable lithology are found throughout the sequence at Site U1562.

4.2.3.2. Igneous petrology

Hole 395C-U1562B was drilled 133 m into basement with a recovery of 48%. In addition, glassy lava fragments and the top of a weathered sheet flow were recovered from the base of Hole 395C-U1562A. The sediment–basement contact is poorly defined. Cores from this site consist of sparsely to moderately olivine phyric pillow lavas with a few massive sheet flow intervals up to 10 m thick (Figure **F9**). Fragmented cryptocrystalline pillow lavas are characterized by curved chilled margins, glassy rinds, and abundant vesicles. Sheet flows have chilled weathered tops and medium grained avesicular interiors. Intercalated peperites and mudstone are common. The peperitic intervals display abundant evidence for lava–sediment mingling, including fragmented basalt clasts with quenched rims and fluidal margins. Thin sections from pillow lavas have abundant

groundmass olivines, sometimes with dendritic forms suggestive of rapid cooling during the eruptive process. The abundance of sediment-rich material at this site suggests that significant amounts of sediment accumulated between eruptions, with preliminary estimates of eruption hiatuses on the order of ~10^5 y.

4.2.3.3. Alteration petrology

The majority of basalt core recovered from Site U1562 is slightly to moderately altered. Intervals of the basalt basement intermixed with carbonate sediment and peperite intervals are highly to completely altered. Alteration is dominantly pervasive, although localized alteration, mainly in the form of fracture halos is also observed. The alteration assemblage is clay+Fe-oxide/oxyhydroxides with minor chlorite and celadonite. Basalt clasts in peperite intervals are mostly altered to palagonite material. Vesicles are dominantly filled with celadonite, Fe-oxide/oxyhydroxides, and calcite with some saponite and minor zeolite. Vesicle fills are commonly mineralogically zoned with mul-

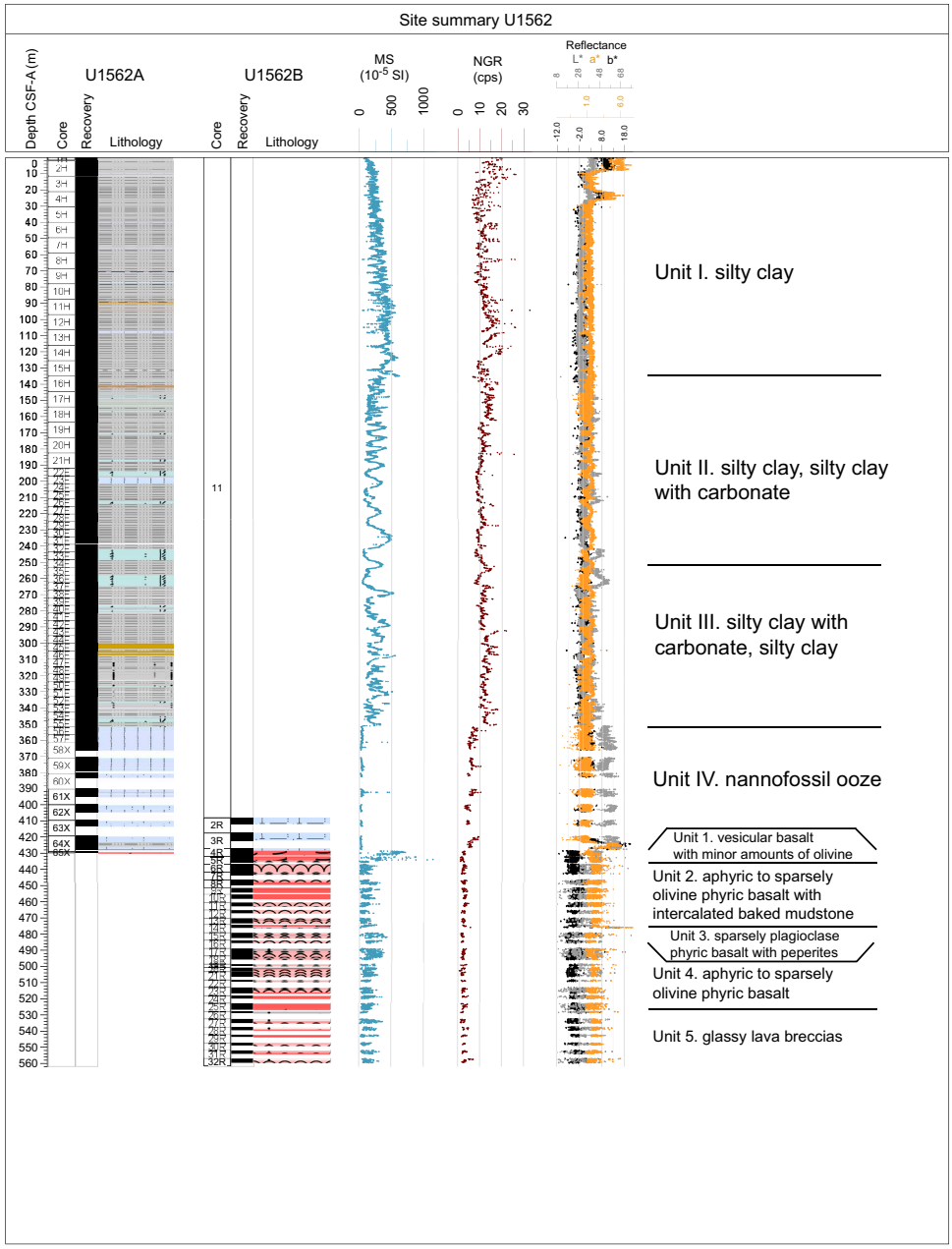

Figure F9. Lithostratigraphic summary, Site U1562. cps = counts per second, Roman numerals = sedimentary units, Arabic numerals = igneous units.

tiple minerals in each. Fracture density in 395C-Hole U1562B is ~21 fractures per meter and is near constant with depth. Fractures are dominantly ≤0.5 mm wide and occur either as isolated, nonconnected fractures or within anastomosing networks. Fracture mineral fills are dominantly carbonate±Fe-oxide/oxyhydroxide with minor clay, chlorite, and celadonite. Peperite and altered carbonate sediment intervals contain complex carbonate filled fracture networks. Fracture alteration halos are up to 2 cm wide from the fracture wall, and are either pale gray, brown, green-gray or green-brown in color.

4.2.3.4. Micropaleontology

At Site U1562 micropaleontological analyses were undertaken on samples from all three holes. Calcareous nannofossils and planktonic foraminifers are generally present in moderate to high abundances, with occasional barren or nearly barren samples. Bolboforms, when present, are generally rare or few. Calcareous microfossil preservation is mostly excellent to very good, with occasional intervals of moderate preservation. The Pleistocene succession is well constrained by biostratigraphy, with eight calcareous nannofossil biohorizons identified in Hole 395-U1562C and five planktonic foraminifer biohorizons identified in both Holes 395C-U1562A and 395-U1562C. No upper Pliocene biohorizons were identified, but one calcareous nannofossil and two planktonic foraminifer biohorizons constrain the lower Pliocene succession. The basal upper Miocene sedimentary succession is also constrained by one calcareous nannofossil and two planktonic foraminifer biohorizons, as well as three bolboform biohorizons. Based on calcareous microfossil biostratigraphy, the bottom of the sedimentary succession is between 11.04 and 11.76 Ma. During the rotary drilling of Hole 395C-U1562B into basement, a substantial interval of sediment (~0.65 m thick) was encountered 45 m into basalt and yielded a well-preserved foraminifer assemblage that is significantly older than the lowermost sample examined from the sedimentary succession.

4.2.3.5. Physical properties

Holes 395C-U1562A and 395-U1562C recovered overlapping stratigraphic sections and, thus, display similar physical properties. Gamma ray attenuation (GRA) bulk density, MS, and NGR increase gradually downhole in the upper 130 m CSF-A with meter-scale oscillations superimposed on this trend (Figure **F10**). The latter two parameters sharply drop at 130 m CSF-A. Below this depth, bulk density displays small variations around an average of 1.6 g/cm^3, and MS and NGR show a more variable pattern: large amplitude variations until ~350 m CSF-A after which core

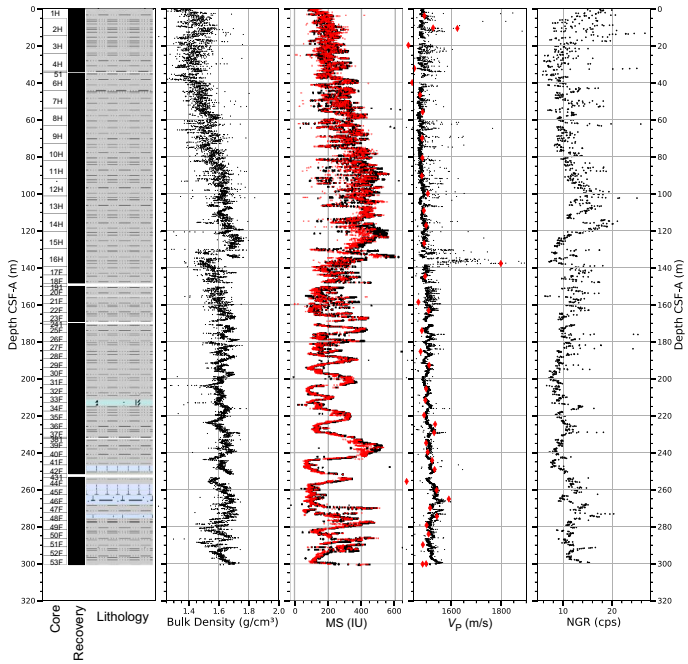

Figure F10. Whole-round physical properties measurements, Hole U1562C. MS: black = WRMSL, red = SHMSL. V_P: black = WRMSL, red diamonds = calipers.

recovery is lower and both measures show lower values. The changes in color properties in the sediments of Holes U1562A and U1562C can be divided in similar stratigraphic intervals as the whole-round property profiles.

In Hole 395C-U1562B, voids and gaps between the core and liners in the basalt sections make the interpretation of their physical properties profile less straightforward. The sedimentary and peperite units in Hole U1562B are apparent in color records, with higher red-green-blue (RGB) a* and b* values.

Caliper measurements of V_P for the sediments from Hole 395C-U1562B are about 1700 m/s, and vary between 4725 and 6053 m/s for the basalt section. Sedimentary V_P values for Hole 395-U1562C average around 1500 m/s. Bulk density values in Hole 395C-U1562A range 1.370–1.673 g/cm^3. Porosity is around 80 vol% and ranges to 65 vol% (average = 70 vol%). Grain density decreases downhole from 2.85 to 2.60 g/cm^3 (average = 2.74 g/cm^3). Thermal conductivity, K, is typically 0.75–1.20 W/(m·K) for the sediments in Holes 395C-U1562A and 395-U1562C, and 1.40–1.80 W/(m·K) for Hole 395C-U1562B.

4.2.3.6. Stratigraphic correlation

Correlation was achieved without gaps from the seafloor through Cores 395C-U1562A-16H and 395-U1562C-17F (155.125 m core composite depth below seafloor, Method A [CCSF-A]). Small coring gaps are present below this depth to ~280 m CCSF-A, but cores can still be tied with some confidence based on the broad cyclic patterns and the comparison with wireline logging MS data from Hole 395C-U1562B. Below Core 395C-U1562A-35F, correlation between holes becomes difficult, probably due to the presence of disrupted sequences (e.g., soft sediment deformation).

4.2.3.7. Paleomagnetism

The sedimentary rocks of Holes 395C-U1562A, 395C-U1562B, and 395-U1562C were demagnetized with a stepwise alternating field cleaning protocol (Figure **F11**). For sediments, an overprint was removed by application of an alternating field of 10 mT. The primary characteristic remanent magnetization (ChRM) was successfully isolated by 25 mT and used to create an age-depth plot for the hole. NRM and MS values both show a variable cyclicity between 160 and 350 m CSF-A. For basalts in Hole U1562B, demagnetization revealed one of two behaviors: 1) 80% magnetization loss before 25 mT or 2) no significant loss of magnetization by 25 mT. The variations in MS coincide with those in NRM intensity and intensity after 25 mT of demagnetization.

4.2.3.8. Geochemistry

Holes 395C-U1562A and 395C-U1562B were analyzed for headspace gas, IW chemistry, and bulk sediment geochemistry. Cores collected from Hole 395-U1562C were analyzed for bulk sediment geochemistry. Methane concentrations are low and range ~0–3 ppmv (Figure **F12**). Ethane is absent in all samples. IW calcium ion (Ca^{2+}) concentrations display a bimodal distribution with highest values near the sediment/water and sediment/basement interfaces. Magnesium ion (Mg^{2+}) concentrations display a generally decreasing trend with depth, with a small increase at the sediment/basement interface. Sulfate ion (SO_4^{2-}) concentrations display a bimodal distribution with seawater-like values at the top and bottom of the sediment column. $CaCO_3$ weight percent generally increases downcore, trending from ~0 to 33 wt% in the top 100 m CSF-A to ~83 wt% near the sediment/basement interface. Bulk sediment generally exhibits low TOC, TN, and TS content.

4.2.3.9. Downhole logging

Logging operations were carried out at Hole 395C-U1562B. A full suite of downhole logs was collected with the triple combo (gamma log, spectral gamma ray, resistivity, density, porosity, MS), FMS-sonic, and VSI tool strings for the sediment and basement sections. In the basement section, the UBI was also deployed. Formation temperature measurements were acquired at Hole 395C-U1562A.

The sedimentary section shows three distinct logging units including multiple subunits. Logging Subunit 1a (0–85 m WSF) was collected through the drill pipe and only collected gamma log and spectral gamma ray. Logging Subunit 1b (85–136 m WSF) shows an increase in the gamma log to peaks up to ~25 gAPI, which are dominated by Th counts. The density increases in this interval

from ~1.2 to ~1.6 g/cm^3. Logging Unit 2 (136–350 m WSF) is characterized by an overall higher cyclic gamma signal (average = 20.5 ± 2.8 gAPI). This cyclic logging response is also observed in the MS, V_S, and porosity measurements of this logging unit. Logging Subunits 2a (136–305 m WSF) and 2b (305–350 m WSF) are differentiated from each other based on the thickness of these logging response cycles. Logging Unit 3 (350–426 m WSF) shows clearly different logging responses with a sharp drop in gamma log and an increase in density with depth from 1.58 to 1.72 g/cm^3. MS is very low (average = 7.9 SI). The image logs of the sedimentary section show layering as well as mottling patterns; however, the frequent ledges and borehole breakouts are influencing the data quality.

Logging Unit 4 encompasses the entire basement section of the hole (426–560 m WSF). The top of Unit 4 is defined by marked changes in resistivity, density, porosity, V_P, V_S, and MS, rather than the gamma log. All logging responses show variability throughout the basement sequence, with increases in MS correlating to increases in V_P, density and resistivity, and decreases in porosity, and vice versa. The image logs as well as the wireline data indicate the potential presence of sedimentary layers intercalated with the basaltic basement. Overall, both image logs are of excellent quality in the basement section of the hole.

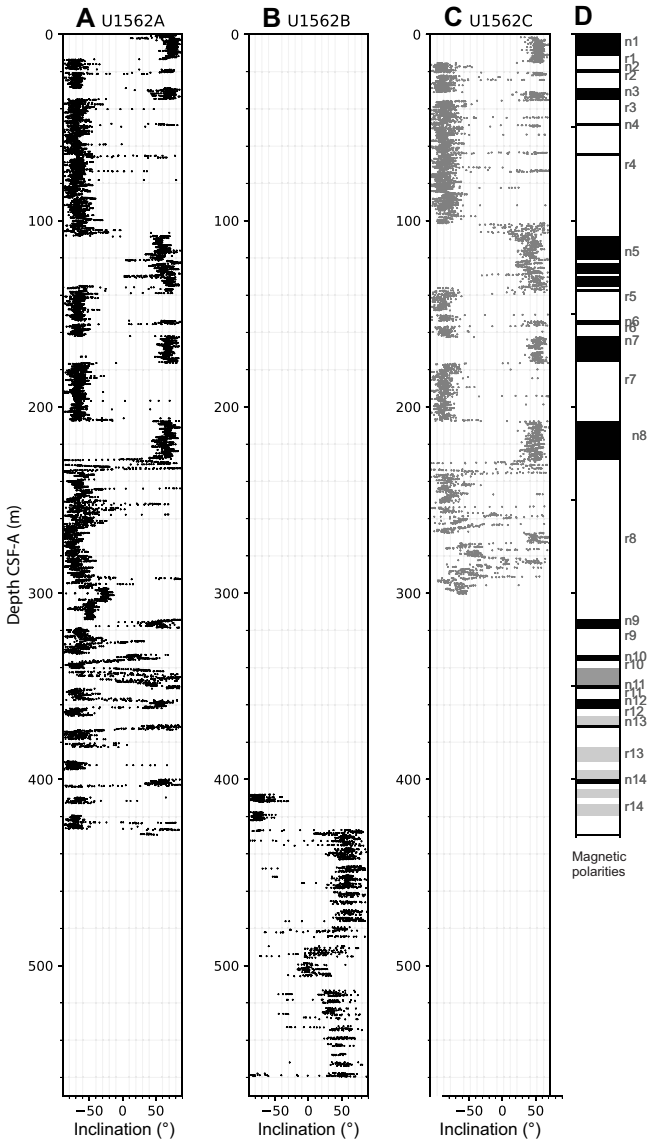

Figure F11. Magnetic inclination data from Holes (A) 395C-U1562A, (B) 395C- U1562B, (C) 395- U1562C, and (D) interpreted polarity chrons.

4.2.3.10. Age model

Magnetostratigraphic and biostratigraphic age constraints for the sedimentary succession in Holes 395C-U1562A and 395-U1562C are combined to create a site age model. Thirteen age datums were chosen to anchor the age-depth model. The succession appears relatively continuous to ~22 m CSF-A. From ~22 to 28.83 m CSF-A, the succession is evidently condensed and/or subject to hiatuses. The age model for the lower part of the succession in Hole U1562A is based on a series of foraminifer, bolboform, and nannofossil biohorizons. These constraints are considered to have a low reliability, for various reasons relating to taxonomic uncertainty, low or variable abundances, and/or age calibration issues. Linear extrapolation of the age model suggests an approximate age of 13.0 Ma for the oldest part of the sedimentary succession overlying basalt.

4.3. Site U1602

4.3.1. Background and objectives

Site U1602 (proposed Site REYK-14B) is located on the eastern margin of Greenland in the North Atlantic Ocean, coinciding with the elongate sedimentary body, Eirik drift (Figure **F1**). Site U1602 is located on a VSR, tentatively identified in free-air gravity anomaly data, that is one of the V-shaped structures that straddle the Reykjanes ridge flanks and whose origin in relation of the Iceland hotspot is debated. The site sits on ocean crust with an age of 49.8 Ma, estimated from magnetic anomalies and plate reconstruction models.

The Reykjanes Ridge flanks are the site of major contourite drift deposits, Björn and Gardar drifts on the eastern flank of the ridge. In contrast, Eirik drift consists of an elongate, mounded contourite deposit that is plastered along the East Greenland margin. These rapidly accumulated contourite drift sediments have the potential to record variations in past climate and ocean circulation on millennial timescales. The sedimentation rate of the drifts can serve as a proxy for deep water current strength, providing information on oceanic gateways to the Norwegian Sea and their potential ties to Iceland mantle plume behavior. The sedimentary section at Site U1602 on Eirik drift has the potential to preserve detailed records of the evolution of the Greenland and Iceland Ice Sheets and of variations in the Western Boundary Under Current. Site U1602 not only complements the sites on the eastern side of the Reykjanes Ridge and the drilling of Björn and Gardar contourite drifts and, paired with the pre-drift record of Site U1564, will recover older sediment, providing insights into the North Atlantic ocean circulation and sedimentation deep into the Cenozoic. Site U1602 is located on Seismic Line JC50-1, obtained in 2010 during RRS *James Cook* Cruise JC50. Sediment thickness at Site U1602 is ~1376 m based on seismic imagery.

The main target for Site U1602 was to obtain a continuous sedimentary record of Eirik drift. Another target was to obtain a sedimentary record throughout the middle Miocene warm period.

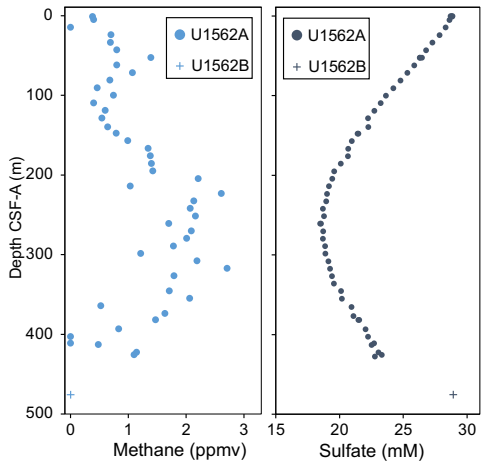

Figure F12. Composite gas analyses of methane concentrations and sulfate concentrations, Site U1562.

A final target, time permitting, was to core into basement. This final objective was not achieved because of time constraints. Cores and data from this site will address the primary science objectives related to mantle behavior, ocean circulation, gateways, and sedimentation.

4.3.2. Operations

Site U1602 (61°11.7138′N, 38°10.8186′W) consisted of five holes, which range 8.8–1365.2 m DSF (Table **T1**). A total of 230 cores were recorded for Site U1602. These cores collected 1444.65 m of sediment over a 1903.8 m cored interval (76% recovery). Two drilled intervals were recorded over a 531.3 m interval. Downhole wireline logging operations were attempted at Hole U1602E and were partially successful. The total time spent at Site U1602 was 19.5 days.

4.3.2.1. Hole U1602A

The ship completed the 350 nmi transit, averaging 11.0 kt, from Site U1562 to Site U1602 at 1701 h on 4 July 2023. The thrusters were lowered, and the ship was in DP mode at 1718 h, marking the start of Site U1602. The bit was spaced out to initiate Hole U1602A (61°11.7138′N, 38°10.8186′W), which was spudded at 0425 h on 5 July. Core 1H recovered 8.8 m of core, establishing a seafloor depth of 2708.6 mbsl. However, Core 1H also recovered part of the "pig," a foam device with metal bristles used to clean rust from the inside of the drill pipe, which disturbed the mudline interval. Hole U1602A was terminated to recover an undisturbed mudline. A total of 8.81 m of core was recovered over an 8.8 m interval (100% recovery).

4.3.2.2. Hole U1602B

Hole U1602B (61°11.7144′N, 38°10.8184′W; 2709.2 mbsl) was spudded at 0535 h on 5 July from the same ship position and Core 1H recovered 5.15 m of core with a good mudline. Coring continued from Cores 2H–16H (5.2–147.7 m DSF). The HLAPC system was deployed for Cores 17F–38F (147.7–251.1 m DSF). Piston coring refusal was reached at Core 38F, which required 80 klb of overpull to free the barrel from the formation. The drill string was pulled from the hole, with the bit clearing the seafloor at 1600 h on 6 July, marking the end of Hole U1602B.

A total of 38 cores were collected from Hole U1602B using the APC and HLAPC, with 262.37 m of core recovered over a 251.1 m interval (104%). Temperature measurements using the third-generation advanced piston corer temperature (APCT-3) tool were collected on Cores 4H, 7H, 10H, and 13H.

4.3.2.3. Hole U1602C

Following Hole U1602B, the vessel was offset 20 m to the north. Hole U1602C (61°11.7253′N, 38°10.8193′W) was spudded at 1920 h on 6 July. Core 1H recovered 7.07 m of core, placing the seafloor at 2710.0 mbsl. Cores 1H–20H (0–180.0 m DSF) were recovered. Within this cored interval, an interval of 2 m was drilled without recovery (64.0–66.0 m DSF; Core 81) to offset coring gaps for stratigraphic correlation. The HLAPC was deployed for Cores 21F–39F (180.0–269.3 m DSF). Piston coring refusal was reached at 269.2 m DSF and the hole was ended. The drill pipe was pulled out of the hole and the bit cleared the seafloor at 0525 h on 8 July, ending Hole U1602C. A total of 38 cores were recovered from Hole U1602C, with 272.63 m of sediment recovered from a 267.3 m cored interval (102% recovery).

4.3.2.4. Hole U1602D

The vessel was offset 20 m to the east of Hole U1602C. Hole U1602D (61°11.7259′N, 38°10.7967′W; 2709.1 mbsl) was spudded at 0805 h on 8 July. Cores 1H–19H advanced from 0 to 175.8 m DSF. APC refusal was reached at 175.8 m DSF and the HLAPC was deployed for Cores 20F–37F and advanced to 260.4 m DSF. The XCB system was used to cut Cores 38X–66X (260.4–540.7 m DSF). The cutting of Core 66X was very slow compared to the other XCB cores. When the core barrel was retrieved it was immediately noticed that the XCB cutting shoe was severely damaged, with large pieces missing. Coring could not continue because the location of the broken metal from the cutting shoe was not known, and therefore Hole U1602D was terminated at 540.7 m DSF. The drill string was pulled from the hole with the bit clearing the seafloor at 1130 h on 11 July. The vessel was offset 20 m south of Hole U1602D and the drill pipe and BHA continued to be pulled up to the rig. At 1645 h, the bit cleared the rig floor ending Hole U1602D. A total of 450.45 m of sediment was recovered from a 540.7 m cored interval (83%) at Hole U1602D.

4.3.2.5. Hole U1602E

The drill string with an RCB BHA and C-4 drill bit was deployed to the seafloor and Hole U1602E (61°11.7150′N, 38°10.7961′W) was spudded at 0630 h on 12 July. A seafloor depth of 2709.2 mbsl was used based upon the offset of Hole U1602B, which recovered the best-preserved mudline core. Hole U1602E was advanced without recovery to 529.3 m DSF, the center bit was retrieved, and rotary coring began. Cores 2R–88R (529.3–1365.2 m DSF) were recovered. Because of expedition time constraints, coring at Hole U1602E was terminated following the recovery of Core 88R and the rig floor began to prepare for downhole wireline logging operations.

The hole was cleaned with 40 bbl of high-viscosity mud. After releasing the RCB bit at the bottom of the hole, the drill pipe was pulled up to 77.8 m DSF. At 0600 h on 22 July, the triple combo was deployed, and the tools run to a maximum depth of 1270 m WSF, at which point the tool string was unable to descend farther into the hole. The calipers were opened for the first pass up the hole and the tool string immediately became stuck. The calipers were closed but the tool remained trapped in the hole. The Hostile Environment Litho-Density Sonde (HLDS) on the triple combo contains a ^{137}Cs radioactive source, making it necessary to recover the tool string.

After attempting to free the tool for over an hour, the wireline cable was cut at the surface and connected to the core winch line to pull on the line with more force. The tool string was briefly freed and ascended 160 m before getting stuck again. The decision was made to run the drill pipe back down the hole and to move the drill pipe over and around the stuck tool string. After some complications, at 1300 h the end of the pipe reached the triple combo tool string at 1079 m DSF. The drill pipe was maneuvered around the tool sting, which was then pulled into the pipe. The tools arrived at the rig floor at 1645 h. The drill string was pulled from the hole with the end of the pipe clearing the seafloor at 2135 h. At 0345 h on 24 July, the end of the pipe cleared the rig floor. The drill floor was secured for transit and the vessel was put into cruise mode at 0409 h, marking the end of Site U1602.

A total of 87 RCB cores collected 450.39 m of sediment from an 835.9 m cored interval (54%) at Hole U1602E. A 529.3 m drilled interval was recorded for the hole.

4.3.3. Principal results

4.3.3.1. Sedimentology

The Holocene to upper Eocene/lower Oligocene sediments cored at Site U1602 are primarily composed of silty clay, silty clay/claystone with nannofossils, nannofossil silty clay/claystone, nannofossil chalk, and sandstone (Figure **F13**). Based on the observations of sediment composition along with attenuation patterns of NGR, MS, and $CaCO_3$ content, Site U1602 is divided into three major lithostratigraphic units (I–III). Unit III consists of two subunits (IIIA and IIIB). The site is dominated by terrigenous components, mainly quartz, feldspar, glass, opaque grains, pyrite, and glauconite with smaller amounts of chlorite and Fe/Mn oxides (Figure **F14**). Biogenic components are dominated by nannofossils, which generally increase downhole. Foraminifers and biosilica are common to rare in Unit I and trace to absent in Units II and III. Sediments at the site contain a wide variety of sedimentary structures such as laminations, graded bedding, alternating grading, crossbedding, flaser bedding, mud drapes, and sand injections. Fractures with slickensides are also present in Units II and III. Bioturbation is generally sparse to moderate in Units I and II. In Unit III, however, bioturbation is generally abundant in the chalk, but absent to sparse in the sandstone intervals.

4.3.3.2. Micropaleontology

At Site U1602, a 1357.99 m interval of upper Eocene to lower Oligocene to upper Pleistocene material was recovered across multiple holes. Micropaleontological analyses were undertaken on sediment samples from Holes U1602B (0–251.43 m CSF-A), U1602C (255.43–264.9 m CSF-A), U1602D (250.31–532.36 m CSF-A), and U1602E (537.07–1357.99 m CSF-A). Biohorizons used in the age model are based on calcareous nannofossils, planktonic foraminifers, and one bolboform species.

Calcareous nannofossils are present in most samples and have variable preservation, which generally worsens with depth below seafloor. A distinct interval where barren samples are more fre-

quent occurs in the Pliocene to early Pleistocene. Seven biohorizons spanning the Pleistocene were identified in Hole U1602B, covering an interval between 0.09 to 1.71 Ma. The top of *Reticulofenestra pseudoumbilicus*, found in Hole U1602D, was the only recorded Pliocene biohorizon. The Miocene was well resolved in Hole U1602E, with fourteen biohorizons covering the interval between 5.53 and 22.9 Ma. Finally, the top of *Reticulofenestra umbilicus*, found in the deepest recovered core catcher sample from Hole U1602E, indicates an early Oligocene (>32 Ma) age for the base of this hole.

Planktonic foraminifers also demonstrate variable preservation (Figure **F15**) that worsens with depth, as well as highly variable abundance. Sample processing became more difficult as sediments became progressively lithified with depth (below ~100 m CSF-A). Despite the difficulties in sample preparation, relatively good biostratigraphic control was achieved across the studied interval. A total of three Pleistocene, four Miocene, and one late Eocene planktonic foraminifer

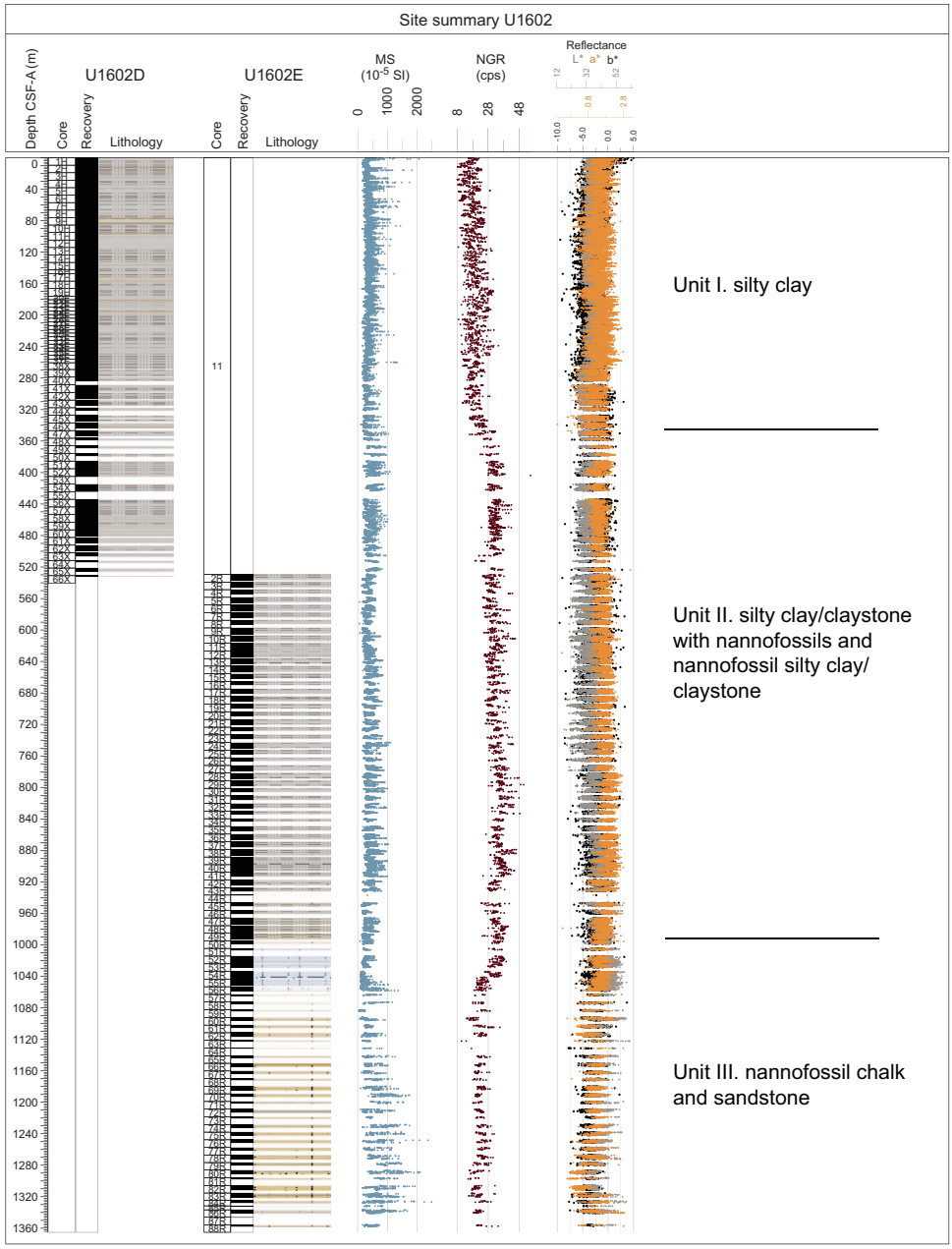

Figure F13. Lithostratigraphic summary, Site U1602. cps = counts per second. Lithostratigraphic units: sedimentary units are shown.

biohorizons were identified across the studied holes. Finally, bolboforms were rare and mostly moderately-to-poorly preserved. Despite that shortcoming, one Miocene biohorizon was recorded in Hole U1602E, using the Top occurrence of *Bolboforma metzmacheri*.

4.3.3.3. Physical properties

Physical property measurements for Site U1602 consist of whole-round and half-round measurements on cores from Holes U1602A–U1602E, including X-ray scan imagery of section halves (Figure **F16**). Discrete physical property measurements were measured from Holes U1602B, U1602D, and U1602E. Density increases with depth and has marked increases at ~350 and ~1050 m CSF-A.

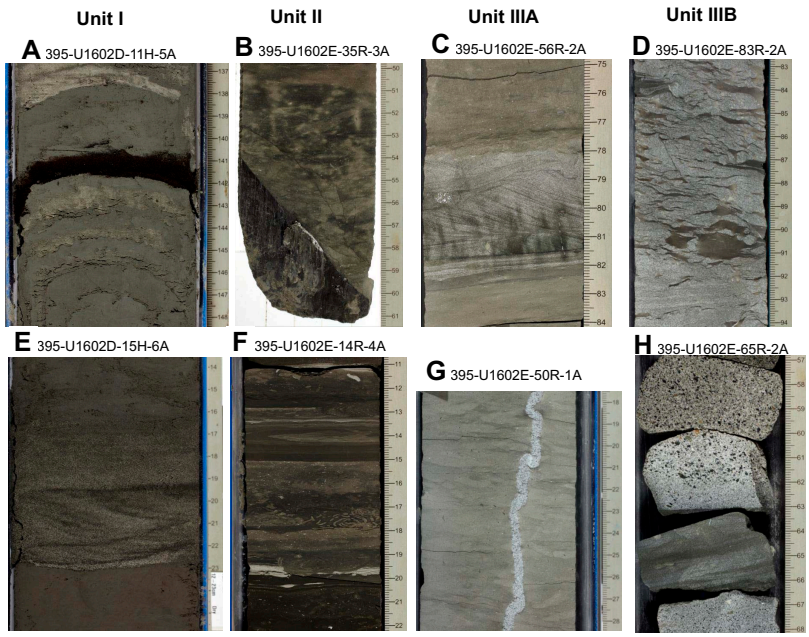

Figure F14. Examples of sedimentary textures and features, Site U1602. A. Silty clay layer with thin bands of silt layers and a dark thick band of glass (ash) layer in the middle. B. Nannofossil silty claystone interval including a fracture with slickensides at the base. C. Nannofossil chalk with an interval of cross bedded siltstone. D. Sandstone containing complex bedform showing rip-up clast or possible flaser bedding features. E. Silty clay with a silt interval displaying cross bedding, graded bedding, and fining-upwards sequence. F. Highly bioturbated silty clay interval with laminations and burrows crosscutting the laminations. G. Nannofossil chalk with sand injection in the middle. H. Laminated siltstone contained within fine- and coarse-grained sandstone.

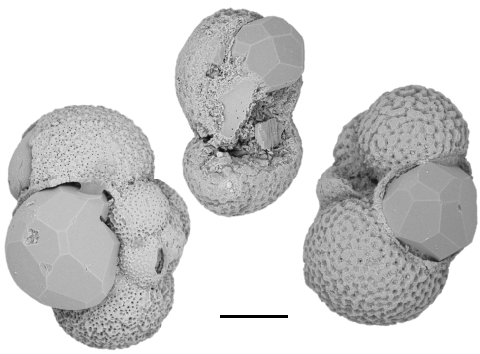

Figure F15. Deformed and broken planktonic foraminifer shells with equant crystal infillings identified as analcime (395-U1602E-25R-CC; 757.61 m CSF-A). Scale bar = 100 µm.

Density values measured on discrete samples are consistently higher than whole-round density values below ~500 m CSF-A, a discrepancy due to the diameter of the core being smaller than that of the liner. Porosity shows the inverse trend of density, with values decreasing with depth and marked decreases occurring at ~350 and ~1050 m CSF-A. Whole- and half-round MS measurements covary, showing meter to decameter-scale fluctuations from the top of the section until ~1050 m CSF-A where more variability is observed. V_P increases sharply from 350 to 650 m CSF-A and increase at a more gentle rate to 950 m CSF-A, after which their measurements show a wider range of values. NGR measurements show an increase from 300 to 400 m CSF-A, and fluctuate downhole to ~950 m CSF-A, followed by an overall decrease and reduced range in values. Red, Green, Blue, L*, and a* show meter to decameter-scale variations between 0 and 1050 m CSF-A. Thermal conductivity of the measured sediments at Site U1602 increases slightly with depth.

4.3.3.4. Stratigraphic correlation

A continuous stratigraphic splice was created from the seafloor to 169.45 m CCSF-A. The continuous splice for the upper 169.45 m CCSF-A includes cores from Holes U1602B and U1602D. Below this depth to ~270 m CCSF-A, there are three small (<1–2 m) gaps in the stratigraphic record. At these intervals, cores were appended to the base of the overlying core.

4.3.3.5. Paleomagnetism

NRM was measured for all sedimentary cores recovered from Site U1602, at a resolution of 2.5 cm. The cores were then demagnetized with a stepwise alternating field cleaning protocol. A set of ~260 discrete samples were collected to confirm the semicontinuous measurements. The inclination measured at the maximum demagnetization step (20, 25, and 30 mT from Holes U1602B, U1602D, and U1602E, respectively) was used to interpret a downcore sequence of normal and reversed polarities. Magnetic polarities from Holes U1602D and U1602E were correlated with the geomagnetic polarity timescale (GPTS) chrons to establish an age-depth trend for Site U1602. Between about 1060 m CSF-A and the bottom of the hole, the NRM intensity and MS decrease, and the paleomagnetic inclinations were not suitable for an univocal magnetostratigraphic interpretation.

4.3.3.6. Geochemistry

Cores taken from Holes U1602B, U1602C, U1602D, and U1602E were analyzed for headspace gas, IW chemistry, and bulk sediment geochemistry. Headspace methane concentrations range 0–328 ppmv (n = 143); low ethane concentrations (<4.6 ppmv) were detected in a subset of the headspace

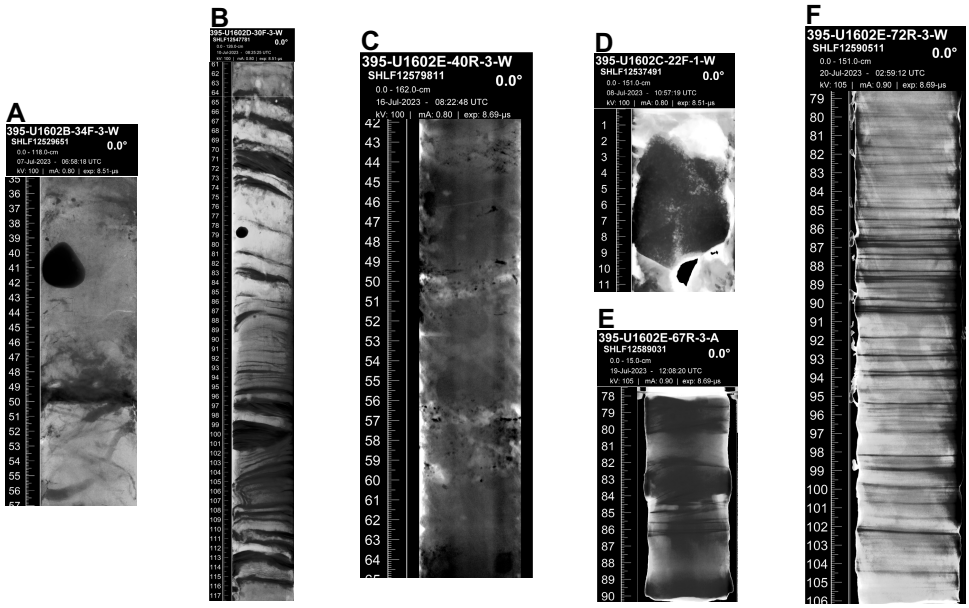

Figure F16. X-Ray scan examples of (A) a dropstone, (B) laminated sequences, (C) IRD deposits, (D) a large clast that is most likely not in situ, (E) cross-bedding, and (F) a laminated interval, Site U1602.

samples (n = 21). The pH and alkalinity of IW display an inverse relationship with depth. Alkalinity is near seawater values (3.68 mM) in the uppermost IW sample (395-U1602A-1H-1, 141–151 cm) and increases to 6.1 mM at ~103 m CSF-A (Sample 395-U1602A-12H-2, 146–151cm) before decreasing to low values (<1.0 mM) below ~320 m (Sample 395-U1602D-44X-2, 123–130 cm). pH is generally constant in the upper ~340 m (7.9 ± 0.1) and increases downhole to 8.9 at ~786 m CSF-A (Sample 395-U1602E-28R-3, 119–131 cm), below which limited IW extracted from the sediment prevented additional pH measurements. IW calcium ion (Ca^{2+}) concentrations display an increasing trend with depth; the highest Ca^{2+} concentrations occur at ~871 m (395-U1602E-37R-2, 103–108 cm). Magnesium ion (Mg^{2+}) concentrations display a general decreasing trend with depth; highest Mg^{2+} concentrations (51.6 mM) occur at top of the sediment column (1.4 m CSF-A; Sample 395-U1602B-1H-1, 141–151cm). Sulfate ion (SO_4^{2-}) concentrations display a decreasing trend downhole and reach the minimum value ~240 m CSF-A (Sample 395-U1602B-35F-2, 145–150 cm). SO_4^{2-} concentrations increase below ~600 m CSF-A to between 5 and 9 mM. Downhole trends in other dissolved elements including barium (Ba), lithium (Li), potassium (K), and silicon (Si) indicate a change in concentrations at around 388 m CSF-A. $CaCO_3$ weight percent generally increases downhole, from ~0 to 30 wt% in the top 100 m CSF-A to as high as ~80 wt% near the bottom of Hole U1602E (Sample 395-U1602E-60R-1, 3–4 cm). Bulk sediment generally exhibits low TOC (<0.7 wt%), TN (<0.2 wt%), and TS ($\lesssim$ 1.0 wt%). Bulk sediment major and minor element concentrations were also analyzed using inductively coupled plasma–atomic emission spectroscopy (ICP-AES) on select samples. Downhole variations in major oxides (e.g., SiO_2, Al_2O_3, TiO_2 K_2O, MgO, and CaO) and trace elements (e.g., S and Sr) show variable concentrations that likely reflect changing lithologies.

4.3.3.7. Downhole logging

After coring operations at Hole U1602E concluded, the hole was prepared for the logging operations. The triple combo tool string became stuck during its first decent downhole and operations to recover the tool were successful, but all further logging operations at Site U1602 were canceled. Therefore, downhole logging data from Hole U1602E consists of a single downhole logging pass that includes measurements of gamma log and spectral gamma ray, formation resistivity, and MS.

Seven logging units are defined for Hole U1602E, the divisions of which are primarily defined by notable changes in the gamma log, and in some instances from other logging responses. Logging Unit 1 (L1) (32–162 m WSF) is characterized by gamma log measurements of ~27.7 gAPI, which fluctuate with depth. Increases in the gamma radiation positively correlates with increases in the thorium and negatively correlates with uranium spectral gamma counts. Logging Unit 2 (L2) (162–340 m WSF) is defined by a step increase in gamma log to ~35 gAPI. MS in Unit L2 has an average measurement of 259 SI and contains meter scale fluctuations. The bottom of Unit L2, top of Unit L3, is defined by an increase in formation resistivity. Logging Unit 3 (L3) (340–588 m WSF) displays an average gamma log of ~47 gAPI and shows meter to decameter-scale fluctuations throughout. Several distinct intervals present very low gamma radiation measurements which correspond to increases in MS. Logging Unit 4 (L4) (588–630 m WSF) is defined by a large ~42 m long fluctuation in gamma log and MS measurements. Logging Unit 5 (L5) (630–1039 m WSF) is defined by an initial decrease in gamma log and an increase in MS and shows fluctuations in gamma log at meter, decameter, and hectometer scales. Logging Unit 6 (L6) (1039–1162 m WSF) is characterized by variable logging responses separated into five subunits. Logging Unit 7 (1162–1280 m WSF) shows meter-scale, fluctuating, cyclical gamma log and MS responses. Below ~1250 m WSF, the values of MS increase; however, this could be a measurement artefact caused by deteriorating hole conditions and not a response to geological variation.

Four downhole temperature measurements were acquired in Hole U1602B (between 33.7 and 116 m DSF). Formation temperature increases from 3.22°C to 10.43°C across this interval. These measurements, along with thermal conductivity, were used to calculate heat flow for the site.

4.3.3.8. Age model

The age model for Site U1602 is based on a combination of paleomagnetic and biostratigraphic age determinations. Some of the biostratigraphic data are only upper or lower depth constraints because rarity and/or variable preservation makes them difficult to locate precisely. There is good agreement between the paleomagnetic and biostratigraphic data sources to the base of Gilbert

Chron C3r. Below that level, the paleomagnetic record continues to follow the expected reversal sequence to the interpreted Base of Subchron C5n.2n (11.06 Ma). However, some of the biostratigraphic data appear to depart from this trend, most likely due to the poor calibration of these events in the high latitudes. The combined biostratigraphic and paleomagnetic record of Site U1602 in this interval will be critical in improving these calibrations in future. The age model is based largely on calcareous nannofossils below this depth and assumes that Oligocene–Miocene global age calibrations are accurate at this location. Planktonic foraminifers suggest that Hole U1602E terminated in the upper Eocene (>34.5 Ma), but that is based on a very poorly preserved assemblage from just one sample near the bottom of the hole.

4.4. Site U1564

4.4.1. Background and objectives

Site U1564 (proposed Site REYK-2A) is located in the North Atlantic Ocean on the eastern flank of the Reykjanes Ridge, south of Iceland (Figure **F1**). Expeditions 384, 395C, and 395 sites comprise a crustal flow line transect across the eastern flank of Reykjanes Ridge. Four sites, U1554, U1555, U1562 and U1563 sampled two pairs of VSRs and VSTs that straddle the flanks of Reykjanes Ridge. Site U1564 is located on the same flow line, on crust with a segmented pattern that does not show evidence for VSRs or VSTs. The estimated basement age at Site U1564 is 32.4 Ma based on magnetic anomalies and plate reconstructions. Basalt samples from this site will provide a record with which to compare samples from VST/VSR pairs, which will provide constraints on the formation of these crustal structures and on hydrothermal alteration of the crust with time.

Site U1564 is also located on Gardar drift, one of the major contourite drifts in the North Atlantic, which has the potential to provide high-resolution, millennial-scale records for paleoceanographic research. The sedimentation rate of this drift can serve as a proxy for deep water current strength, providing information on oceanic gateways and their potential ties to mantle plume pulses. ODP Site 983 was cored on Gardar drift, obtaining a sedimentary sequence back to ~2 Ma (early Pleistocene). Cores at Site U1564 extend this record back to the Oligocene epoch.

One main target for Site U1564 was to obtain basalt core from crust not showing traces of VST/VSR structures. Another main target was to obtain a continuous sedimentary record of the Gardar drift. Cores and data from this site will address all three of the primary science objectives: (1) crustal accretion and mantle behavior; (2) ocean circulation, gateways, and sedimentation; and (3) time-dependent hydrothermal alteration of oceanic crust.

The operational objectives for this site were to core the sedimentary section using the APC, XCB, and RCB systems, install a reentry system with casing to 600 m DSF, use the RCB to core ~130 m into the basement, and use downhole wireline tools to log the borehole.

4.4.2. Operations

4.4.2.1. Expeditions 395C and 395

4.4.2.1.1. Site U1564

Site U1564 (proposed Site REYK-2A) (59°51.0366′N, 23°15.9858′W) consisted of six holes drilled during Expeditions 395C and 395. These holes range 8.8–1169.7 m DSF (Table **T1**). A total of 255 cores were recorded for Site U1564. These cores collected 1881.5 m of sediment and 114.2 m of basalt over a 2155.1 m cored interval (93% recovery).

The APC system was used to collect 65 cores over a 609.0 m interval with 636.1 m of core recovered (104% core recovery). The HLAPC was deployed for 24 cores and recovered 117.76 m of sediment from a 112.8 m interval (104%). The XCB system was deployed over a 861.6 m long interval. The 51 XCB cores recovered 807.67 m of sediment (94%). The RCB system was deployed for 75 cores and recovered 434.15 m of sediment and basalt across a 571.7 m interval (76%). Downhole wireline logging operations using the triple combo tool string, FMS-sonic, and UBI took place at Holes U1564C and U1564F.

The total time spent at Site U1564 was 21.69 days across Expeditions 395C and 395.

4.4.2.2. Expedition 395C

4.4.2.2.1. Hole U1564A

The vessel arrived at Site U1564 at 1748 h on 30 July 2021. The thrusters were lowered, the ship entered DP mode, and the drill string was made up with an APC/XCB BHA. The drill string was run to 2220.0 mbsl to spud Hole U1564A (59°51.0377′N, 23°16.0071′W), ~20 m west of the site coordinates. The exact site coordinates were to be reserved for future reentry system and casing installation during Expedition 395. Hole U1564A was initiated at 0245 h on 31 July and Core 1H recovered a full core (9.89 m), prohibiting the establishment of the seafloor depth.

4.4.2.2.2. Hole U1564B

The ship was offset 20 m to the east—unintentionally locating the ship directly over the site coordinates—and Hole U1564B (59°51.0372′N, 23°15.9868′W) was spudded at 0342 h on 31 July. Core 1H recovered 7.22 m of sediment, placing the seafloor at 2207.9 mbsl. Coring continued through Core 3H when the error in the ship's offset was noted and operations at Hole U1564B were terminated. The bit cleared the seafloor at 0630 h, ending Hole U1564B. A total of 26.81 m of core was collected over a 26.2 m cored interval (102% recovery).

4.4.2.2.3. Hole U1564C

The ship was offset 20 m west, over the Hole U1564A coordinates, and Hole U1564C (59°51.0374′N, 23°16.0087′W) was spudded at 0707 h on 31 July. The seafloor depth was calculated at 2208.1 mbsl, based on the recovery of Core 1H (7.02 m). Coring continued with the APC system recovering Cores 2H–17H (7.0–159.0 m DSF). APC refusal was reached and Cores 18F–35F advanced from 159.0 to 243.6 m DSF. Cores 36X–75X were collected to 628.9 m DSF. Following Core 75X, the crew began pulling up the drill string in preparation for downhole logging operations using the triple combo tool.

The drill pipe was raised until the bit was at 80.6 m DSF. The triple combo logging tool string was made up and at 0250 h on 4 August the tool string was deployed. The triple combo made two passes of the borehole, was recovered at 0930 h, and broken down. The FMS-sonic tool string was made up, deployed to the base of the hole, and made a single pass imaging the borehole wall. The downhole logging equipment was put away and the logging tools moved to the helideck. The rig floor crew began pulling up the pipe, with the bit clearing the seafloor at 1845 h. At 0106 h on 5 August the ship switched from DP mode to Bridge control, ending Site U1564. The ship began the 293 nmi transit to Reykjavík, Iceland. In all, 618.71 m of core was recovered from Hole U1564C (98.4%).

4.4.2.3. Expedition 395

4.4.2.3.1. Hole U1564D

Following a 1349.5 nmi voyage from Ponta Delgada, Portugal, at an average speed of 11.2 knots, the vessel arrived on site at 1424 h on 21 June 2023. The thrusters were lowered and secured at 1456 h on 21 June and the ship was fully in DP mode at 1502 h. Hole U1564D (59°51.0483′N, 23°16.0080′W; 2208.2 mbsl) was spudded at 0500 h 22 June with the first core on deck at 0530 h.

Piston coring using the APC advanced from Core 395-U1564D-1H through 22H (0–209.0 m DSF), with 218.87 m of core recovered (105%). APC refusal was reached at Core 22H, which was drilled over with the drill bit to recover the core barrel. The HLAPC system was deployed for Cores 23F–29F (209.0–239.2 m DSF). The stratigraphic correlators requested a 2 m drilled interval (26-1), from 223.2 to 225.2 m DSF, to offset coring gaps to assist with stratigraphic correlation. The XCB using a polycrystalline diamond compact (PDC) bit and cutting shoe was deployed. Coring with the XCB system continued with Cores 30X–74X (239.2–657.3 m DSF). The rate of penetration slowed and recovery in the final three cores (72X–74X) was lower than the rest of the hole (33%), due to the water jets in the cutting shoe getting clogged with sediment. The hole was terminated at a final depth of 657.3 m DSF. A total of 73 cores were collected in Hole U1564D over a 655.3 m interval and recovered 632.42 m of core (97%).

The drill pipe was pulled out of the hole, with the bit clearing the seafloor at 2015 h on 25 June 2023, ending Hole U1564D. In all, 632.42 m of core was recovered from Hole U1564D (97%).

4.4.2.3.2. Hole U1564E

The vessel was offset 20 m east and Hole U1564E (59°51.0485′N, 23°15.9876′W) was spudded at 2306 h on 25 June. Core 1H recovered a 5.8 m mudline core, establishing a seafloor depth of 2207.3 mbsl. Coring continued from 5.8 to 205.3 m DSF with Cores 1H–22H. Cores 23X–28X extended the hole to 263.5 m DSF. Following Core 28X, the decision was made to end the hole. A total of 273.7 m of sediment was recovered from the 263.5 m cored interval at Hole U1564E (104%).

At 0030 h on 27 June, the drill bit cleared the seafloor and at 0545 h the bit cleared the rig floor. At 0640 h, the ship was secured for transit. The thrusters were raised and the transit to Site U1554 began at 0700 h, ending Hole U1564E. In all, 273.7 m of core was recovered from Hole U1564E (104%).

4.4.2.3.3. Hole U1564F

The vessel completed the 448 nmi transit from Site U1602 to Site U1564 at 2030 h on 25 July. The thrusters were lowered and the ship was put into DP mode at 2106 h, resuming operations at Site U1564.

The rig crew made up the hydraulic release tool casing running stand. The weather was forecast to deteriorate throughout the day with ~5 m heave, preventing the assembly of the casing and reentry system. The vessel began waiting on weather at 0200 h on 26 July.

At 1500 h on 26 July the Icelandic Coast Guard offshore patrol vessel, *Þór* (*Thor*), arrived to deliver the Schlumberger severing devices and other supplies. After waiting nearly 2 h, the transfer was postponed due to weather. *Thor* returned the next day at 0823 h for the transfer of severing tools, supplies, and fresh produce. *Thor* pulled alongside the vessel and the portside aft crane was used to transfer six pallets onto the helideck starting at 0902 h. By 0919 h, the transfer was complete, and *Thor* departed at 0925 h.

The rig crew began preparing for the casing installation operations on 27 July immediately following the departure of *Thor*. The casing and reentry system was assembled. At 1200 h on 28 July, the moonpool doors were opened and the reentry system was lowered below the ship. The rig crew began making up the drill string to 2180 mbsl. The subsea camera system, along with Niskin water samplers and the CTD tool, were deployed at 1730 h. The top drive was picked up and the bit spaced out to initiate Hole U1564F at 2125 h on 28 July. The casing string was drilled to 550 m DSF and the bit advanced to 553.5 m DSF. The go-devil was pumped down the pipe to release the casing stinger from the reentry system. The VIT camera system was retrieved, and the drill string was pulled to surface. The bit cleared the seafloor at 1440 h on 29 July and the rig floor at 2230 h.

After breaking down the reentry equipment, the RCB BHA was made up with a C-4 drill bit. The drill pipe was run to 1598.7 mbsl. The VIT camera system, with the CTD recorder and two Niskin bottles attached, were deployed through the moonpool at 0845 h on 30 July. The drill string continued to be lowered to several meters above the seafloor. The reentry cone for Hole U1564F was found and the bit reentered the hole at 1052 h on 30 July. The subsea camera was recovered while the drill string was lowered to the base of the hole and the top drive was picked up. The center bit was deployed, and the hole was conditioned with 20 bbl of high-viscosity mud. The hole was advanced without recovery from 553.4 to 598.0 m DSF. The center bit was retrieved and an RCB core barrel deployed.

Cores 395-U1564F-2R through 43R (598.0–995.8 m DSF) were recovered and Core 4R had no recovery.

The basaltic basement was reached at ~997.2 m DSF in Core 395-U1564F-44R. This core recovered 7.03 m of material (74%), including 1.43 m of sediment and the remainder basalt. Coring continued with Cores 45R–49R (1005.3–1039.2 m DSF). Beginning with Core 46R, all cores were half advances (4.7 or 5.0 m), except for Core 48R.

Following Core 395-U1564F-49R, the drill bit had reached 59.7 rotating hours and the drill string was pulled out of the hole to change the bit. At 1640 h on 4 August the bit cleared the seafloor, and the vessel was offset 20 m east of Hole U1564F. At 2030 h the bit cleared the rig floor. The drill pipe and BHA were run from the ship to near the seafloor for reentry into Hole U1564F. At 0315 h on 5

August the VIT camera was deployed to guide the hole reentry. The bit was spaced out and, after nearly 2 h of searching for the reentry cone, the bit entered Hole U1564F at 0725 h. The drill pipe was run in the hole and the subsea camera retrieved. At 1115 h, coring resumed.

Cores 395-U1564F-50R through 76R (1039.2–1169.7 m DSF) were retrieved. Hole U1564F was terminated at a final depth of 1169.7 m DSF. A total of 434.15 m of core was recovered from a 571.7 m interval (76%) from Hole U1564F. The recovery in the basement section was high (66%) with 114.2 m of core recovered over 172.4 m. Two drilled intervals, totaling 598.0 m, were recorded.

Following the completion of coring operations, the hole was cleaned with a mud sweep. The drill pipe was pulled out of the hole. At 0215 h on 9 August, the subsea camera was deployed and descended to near the seafloor. The bit cleared the seafloor at 0325 h, and the vessel was offset 20 m from Hole U1564F. The mechanical bit release sleeve was activated, and the drill bit fell to the seafloor. The end of the drill pipe reentered Hole U1564F at 0625 h. The end of the pipe was positioned at 59.3 m DSF in the casing string for logging operations.

The triple combo tool string was rigged up and deployed to the base of the hole (1169.7 m DSF). On the upwards pass, the Accelerator Porosity Sonde (APS) malfunctioned and porosity measurements were not collected. Following a complete pass of the hole, the triple combo was pulled to the rig floor and broken down. The FMS-sonic was made up and deployed in the hole. On the downward pass, the Dipole Sonic Imager (DSI) malfunctioned and was not used. Two passes of the borehole were successfully made with the FMS-sonic tool string. The UBI was run to 1164.7 m WSF, 5 m above the base of the hole. The basement section was first logged at high resolution to test the image quality and because there was enough time in the program. The UBI was then lowered back to 1164.7 m WSF and the entire hole was logged at a lower resolution scan. The rig crew pulled the drill pipe out of the hole, with the bit clearing the seafloor at 1525 h on 10 August. The BHA was broken down and the end of the pipe reached the rig floor at 2130 h. The vessel was secured for transit and at 2206 h the vessel was switched from DP to cruise mode, ending Site U1564. The thrusters were raised the vessel began the 293 nmi transit to Reykjavík at 2230 h on 10 August.

4.4.2.3.4. Transit and end of Expedition 395

Following a 293 nmi transit, the vessel reached the pilot station and the pilot boarded at 0705 h on 12 August. *JOIDES Resolution* came into Skarfabakki Harbour in Reykjavík, Iceland. The first line ashore at Vatnagardsbakki Berth was at 0812 h, marking the end of Expedition 395.

4.4.3. Principal results

4.4.3.1. Sedimentology

The Holocene to lower Oligocene sediments cored at Site U1564 are primarily composed of silty clay, silty clay/claystone with nannofossils, nannofossil silty clay/claystone and nannofossil chalk with silty clay (Figure **F17**). Based primarily on lithologic observations and sediment composition, alongside NGR and $CaCO_3$ measurements, Site U1564 is divided into two major lithostratigraphic, Units I and II. Each Unit is further divided into three subunits.

In Unit I, Subunit IA is dominated by gray silty clay, with a variable but generally minor biogenic component. The biogenic component is dominated by nannofossils, and foraminifers and siliceous microfossils are also observed. $CaCO_3$ weight percent is variable in this subunit. Several prominent glass layers are present, dark green banding is observed throughout, and some sharp contacts are observed intermittently. Subunit IB is similarly dominated by gray silty clay and silty clay with biogenics. In addition to thin glass layers and intermittent sharp contacts, pyritization of burrows and halos around burrows are observed. Subunit IC is dominated by dark gray silty clay; this subunit contains the least biogenic carbonate of all units in Site U1564 (supported by smear slide analysis and $CaCO_3$ weight percent).

Unit II is marked by an increase in carbonate content and a transition to nannofossil chalk with silty clay. In this unit glass layers, sharp contacts and dark banding continue to be present. Fractures with slickensides and/or calcite veins, and soft sediment deformation features are also observed (Figure **F18**). Subunit IIA is dominated by dark gray silty clay with nannofossils inter-

bedded with nannofossil chalk. There is a significant increase in the variability of both biogenic carbonate and $CaCO_3$ weight percent, coinciding with cyclical color grading of sediment beds. Subunit IIB is dominated by greenish gray nannofossil chalk and dark gray silty nannofossil chalk. Subunit IIC is dominated by gray nannofossil chalk with silty clay, with some intervals of silty nannofossil chalk. Near the base of the sedimentary sequence, red and pink nannofossil chalks become interbedded. Evidence for hydrothermal mineralization is observed.

4.4.3.2. Igneous petrology

Site U1564 recovered the oldest oceanic crust drilled during this expedition (~32.3 Ma). Site U1564 is located in faulted abyssal hill topography that formed when the ridge axis was segmented by a series of transform offsets. The sediment/basement interface was encountered at 997 mbsf. Basement was drilled to 1170 m CSF-A at Hole U1564F, penetrating 172.4 m of basalt, of which 114.2 m of core was recovered (66%). The bulk of this core consists of continuous sheet flows that

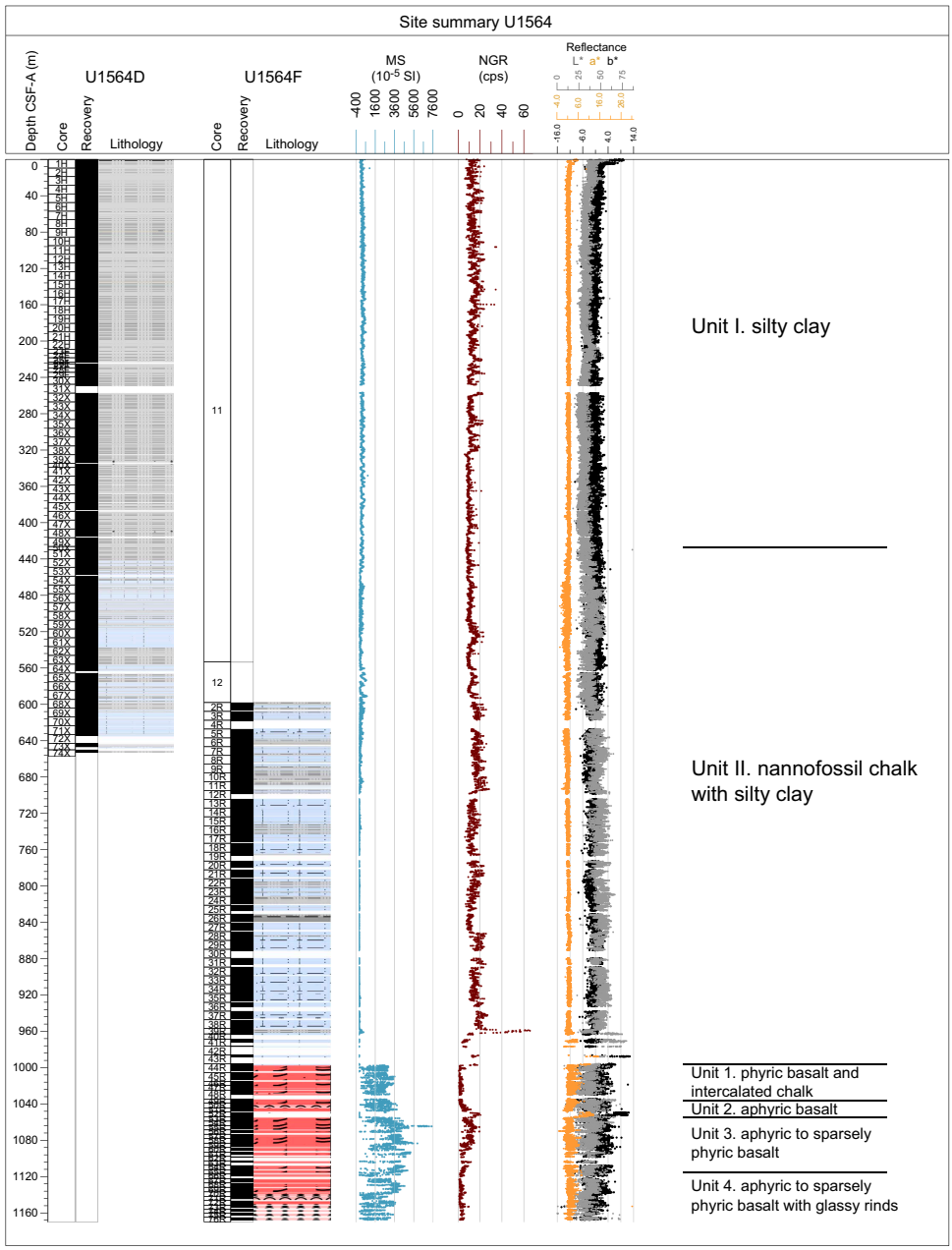

Figure F17. Lithostratigraphic summary, Site U1564. cps = counts per second, Roman numerals = sedimentary units, Arabic numerals = igneous units.

are moderately to highly altered, with sparsely plagioclase phyric basalt and occasional clinopyroxene microphenocrysts. The fine- to medium-grained groundmass consists of plagioclase, clinopyroxene and opaque minerals. A 4 m thick dusky red sediment layer was encountered at ~1050 m CSF-A. In the bottom ~40 m of the cored section, pillow lavas become more abundant, with chilled margins and occasional glassy rinds. Filled fractures and complex anastomosing veins are common throughout the hole.

4.4.3.3. Alteration petrology

The majority of basalt core recovered from Site U1564 is completely or highly altered. Alteration is dominantly pervasive though localized alteration mainly in the form of fracture halos occurs throughout the basalts. Alteration intensity is observed to be slightly higher in sheet flows than in pillow lavas. The basalt alteration assemblage is Fe-oxide/oxyhydroxides + celadonite + clay with minor, localized chlorite (Figure F19). Vesicles are dominantly filled with celadonite, calcite, Fe-

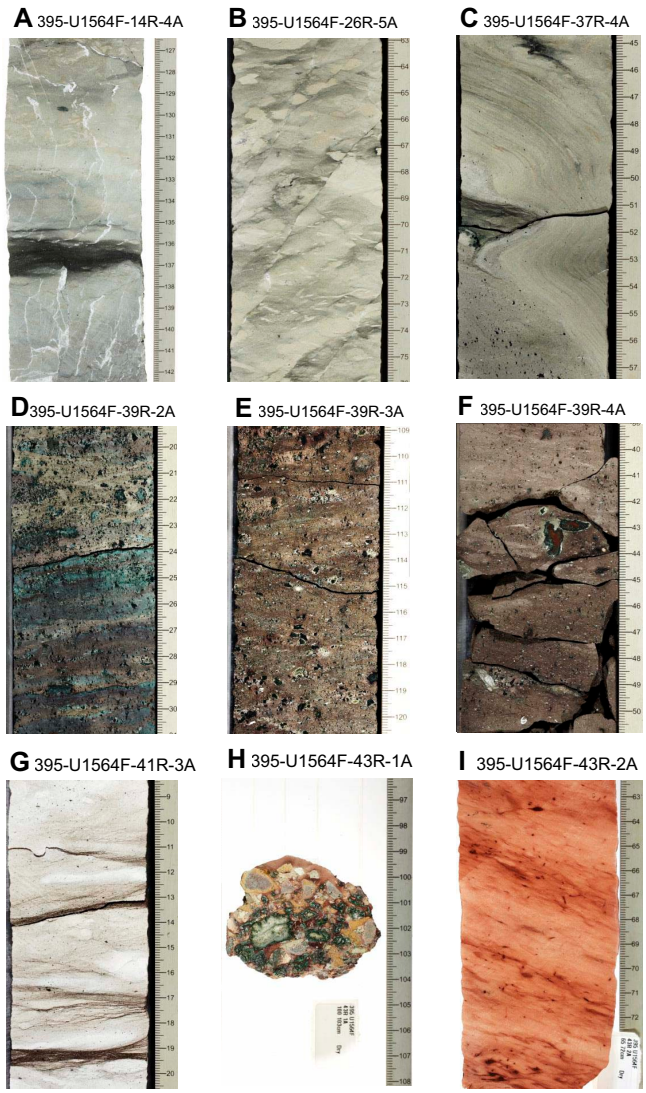

Figure F18. Examples of fracturing, soft sediment deformation, glauconite-rich interval, stylolites, malachite-bearing breccia, and pink chalk, Hole U1564F. A. Network of thin, calcite-infilled fractures. B. Parallel fractures. C. Well-defined soft sediment fold. D–F. Brightly colored sediment with abundant glauconite pellets. This layer coincides with a strong peak in NGR values. G. Stylolites (thin dark brown bands) within nannofossil chalk. H. Breccia with clasts of malachite and malachite-rimmed calcite, along with other minerals associated with hydrothermal alteration such as jarosite. The matrix of this breccia is pinkish nannofossil chalk, as seen in I.

oxide/oxyhydroxides, some saponite and minor zeolite. Vesicle fills are commonly mineralogically zoned with multiple minerals in each. Fracture density in Hole U1564F is ~23 fractures per meter and increases gradually with depth. Fractures are dominantly <1 mm wide and occur mostly within complex crosscutting networks. Fractures up to 3.4 cm wide are more common in the upper intervals of basalt. Fracture mineral fills are dominantly carbonate ± Fe-oxide/oxyhydroxide ± celadonite with minor clay. Chlorite fracture fill occurs in specific intervals and quartz is sporadically observed as a late fill in some mineralogically layered fractures. Fracture alteration halos can be >15 cm wide, and are red, brown, green-gray, to green-brown in color.

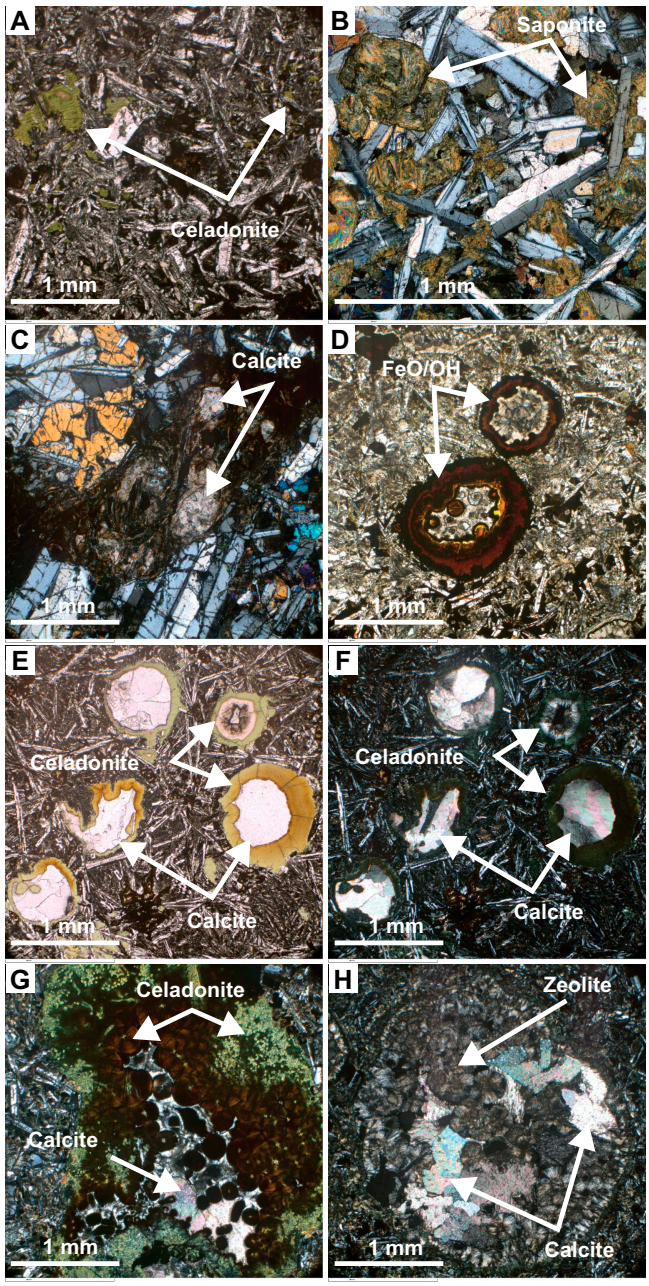

Figure F19. A. Celadonite alteration in groundmass (395-U1564F-49R-1, 145–147 cm; plane-polarized light [PPL]). B. Saponite alteration (395-U1564F-45R-2, 60–62 cm; cross-polarized light [XPL]). C. Calcite replacement in crystals (395-U1564F-61R-2, 86–89 cm; XPL). D. FeO/OH-rimmed vesicles (395-U1564F-63R-1, 40–43 cm; PPL). E. Yellow and green celadonite-rimmed vesicles filled with calcite (395-U1564F-73R-1, 21–23 cm). F,G. Zoned vesicle containing, from the rim to the center, green celadonite, brown celadonite spherules and calcite in (F) XPL and (G) PPL (395-U1564F-53R-2, 114–116 cm). Vesicle filled with zeolite and calcite (395-U1564F-63R-1, 99–102 cm; XPL).

4.4.3.4. Micropaleontology

At Site U1564, a 997.23 m long interval of lower Oligocene to upper Pleistocene sediments were recovered across multiple holes. Planktonic foraminifers are common to dominant in most samples examined except where quartz grains and rock fragments predominate and their preservation is very good to excellent to ~530 m CSF-A. Below that level the sediment becomes progressively more lithified and the foraminifers are mostly infilled by calcite, although they continue having moderate to good preservation up to ~800 m CSF-A. Seven early Pliocene to Pleistocene biohorizons, three Miocene biohorizons, and two Oligocene biohorizons were recorded. The last sample of the regular succession above basement has an assemblage that indicates an early Oligocene age (32.2–27.29 Ma), and the assemblage in the sedimentary layer recovered between the basement succession points to an age between 33.8 and 32.2 Ma.

Similar to the planktonic foraminifers, calcareous nannofossils are present in almost all samples observed, ranging from few to dominant in abundance and with very good to poor preservation. Preservation worsens with depth in the succession. Ten Pleistocene biohorizons were identified, only one Pliocene biohorizon, and eleven Miocene biohorizons spanning the interval between 5.53 and 17.65 Ma. Oligocene assemblages are present below ~920 m CSF-A, characterized by the presence of *Cyclicargolithus abisectus*, with the lower Oligocene biohorizon Top *R. umbilicus* at ~987 m CSF-A constraining the base of the sedimentary succession to be older than 32.02 Ma.

4.4.3.5. Physical properties

Physical properties measurements for Site U1564 consist of whole-round and half-round measurements on cores from Holes U1564B through U1564F. Discrete physical property measurements were measured from Holes U1564D, U1564E and U1564F. Whole-round density measurements show an increase with depth with marked increases at ~550, ~700 m and ~1000 m CSF-A (the sediment/basement interface). Density measured on discrete samples is consistently higher than those measured on whole-round sections, below ~700 m CSF-A. Whole-round and point MS measurements covary, showing meter to decameter-scale fluctuations throughout the sedimentary section. Below 700 m CSF-A, MS drops dramatically to values below 10 IU. V_P from whole-round measurements increases between 450 and 650 m CSF-A, below which the measurements were constrained to caliper measurements due to the diameter of the RCB core not filling the core liner. Below 650 m CSF-A in the sediment interval, velocities increase from 2200 to 3000 m/s. Caliper-derived velocities in the basalts were measured on the orthogonal direction using the paleomagnetic cubes; these velocities vary between 3600 and 6000 m/s. NGR measurements show an increase between 600 and 700 m CSF-A and then fluctuates between 700 to ~1000 m CSF-A. NGR is generally lower in the basaltic record. RGB L*, and a* show meter to decameter scale variations with depth between 0 and 450 m CSF-A, below which the data display higher amplitude variability. RGB measurements have lower values in the basaltic records, averaging around 50. L* shows lower values in the basalts, averaging around 40, and L* and b* display a similar range of values to the sediment intervals.

4.4.3.6. Stratigraphic correlation

The stratigraphic splice for Site U1564 contains two long uninterrupted intervals that are complete, with a ~200 m long interval in between that has several gaps. In Cores 395-U1564E-1H through 23X, a continuous splice was constructed using only Holes 395-U1564D and 395-U1564E to 239 m CCSF-A. The lowermost, continuous part of the Site U1564 shipboard splice was constructed using material from Holes 395C-U1564C and 395-U1564D to 674.71 m CCSF-A. Between these intervals, several gaps are unavoidable and cores from Holes 395C-U1564C, 395-U1564D and 395-U1564E were positioned to our best judgement, with additional guidance from the downhole wireline MS logging profile from Hole 395C-U1564C.

4.4.3.7. Paleomagnetism

NRM was measured for sedimentary cores recovered from Holes U1564A, U1564B, U1564C, U1564D, U1564E and U1564F. The cores from Holes U1564B, U1564C, and U1564E were then demagnetized with a stepwise alternating field cleaning protocol with a resolution of 5 cm, and Holes U1564A, U1564D, and U1564F with a resolution of 2.5 cm. A set of about 150 discrete samples were collected to confirm the semicontinuous measurements. The inclinations measured at the demagnetization step of 20 mT from Holes U1564D and U1564F were used to interpret a

downcore sequence of normal and reversed polarities. Cores 395-U1564F-10R through 30R of the half-core measurements and for all the discrete samples we used in the principal component analysis for interpreting the paleomagnetic signal. The change in lithology below about 750 m CSF-A corresponds to a decrease of the NRM intensity and the magnetic susceptibly, together with the deterioration quality of the paleomagnetic signal. Below 997 m CSF-A, the sediment/rock interface between Sections 395-U1564F-44R-1A and 44R-2A, marks a three-fold increase in the intensity of the NRM, of the MS but the alteration of the basement rocks causes a deterioration of the paleomagnetic signal. Hence, between about 760 m CSF-A and the bottom of the hole the paleomagnetic inclinations were not suitable for an univocal magnetostratigraphic interpretation. Magnetic polarities from Holes U1564D and U1564F were correlated with the GPTS chrons to establish an age-depth trend for Site U1564.

4.4.3.8. Geochemistry

Cores collected from Site U1564 were analyzed for headspace gas, IW chemistry, and bulk sediment geochemistry. Headspace gas analyses were conducted at Holes U1564A, U1564B, U1564C, U1564D, and U1564F; methane concentrations are variable and range ~0–1260 ppmv. Ethane, at concentrations lower than 94.6 ppmv, was present in Holes U1564C, U1564D, and U1564F below 510.31 m CSF-A.

Material from Holes U1564D, U1564E, and U1564F was analyzed for IW chemistry and bulk sediment geochemistry. Calcium ion (Ca^{2+}) concentrations generally increase, and magnesium ion (Mg^{2+}) concentrations decrease with depth. Sulfate ion (SO_4^{2-}) concentrations decrease from seawater-like values at the top of the sediment column <1 mM at 173.87 m CSF-A, with a small increase in concentration below 607.12 m CSF-A. $CaCO_3$ weight percent generally increases downcore, trending from an average of 13.3 ± 9.6% through Sample 395-U1564D-52X-2, 141–151 cm (442.31 m CSF-A), to an average of 35.4 ± 20.6% for the remaining sediment samples to the sediment/basement interface. Bulk sediment generally had low TOC, TN, and TS content.

4.4.3.9. Downhole logging

After coring operations concluded at Holes 395C-U1564C and 395-U1564F, the holes were cleaned with a mud sweep and the drilling mud displaced with seawater before logging operations started. Hole 395C-U1564C was logged with the triple combo and the FMS-sonic tool strings from the seafloor to ~630 m WSF. Hole 395-U1564F was logged from ~550 to 1160 m WSF to allow for some data overlap with Hole 395C-U1564C. For Site U1564, six logging units have been identified from first order variations in the wireline measurements, predominantly using observable changes in the gamma ray log, and in places using other logs such as resistivity, MS, and density. Logging Subunit 1a encompasses data collected through the drill pipe, and Logging Subunit 1b records the open hole logging responses of Logging Unit 1. Logging Unit 1 is defined by gamma log measurements of 19 ± 3 gAPI and densities ranging 1.2–1.6 g/cm^3. Logging Unit 2 (L2) (108–318 m WSF) is defined by an increase in gamma log to an average value around 21 ± 3 gAPI, spectral gamma ray that shows several large district peaks in thorium counts, and an increase in MS (average = 117 ± 45 SI), the latter of which increasingly fluctuates with depth. Logging Unit 3 is marked by a decrease in gamma radiation, and gradually increasing V_P and V_S. This unit is divided into two subunits based on changes in the frequency of fluctuations observed in the magnetic susceptibly. A large distinct peak in uranium radiation at ~529 m WSF is observed in Logging Subunit 3b. Logging Unit 4 (L4) (560–957 m WSF) is marked by an increase gamma radiation, resistivity, MS, and density. This logging unit contains three subunits defined by variations in gamma radiation. Logging Unit 5 is marked by a large spike in gamma log as well as an increase in resistivity and density. Logging Unit 6 marks the transition from sediment to basaltic basement which sees a decrease in gamma log and thorium counts in the spectral gamma ray log, and large increases in resistivity and density. FMS image logging of Hole U1564C is of good quality and alternating conductive and resistive bedding features can be observed. FMS and UBI image logging in the sediment and basement lithologies of Hole U1564F are also of good quality and show multiple sedimentary and structural geology features.

4.4.3.10. Age model

The age model is based mainly on a combination of paleomagnetic and biostratigraphic age determinations from Holes U1564D and U1564F, with additional biostratigraphic constraints from

Hole U1564C. Fourteen tie points were selected that divide the stratigraphy into a series of intervals characterized by significantly different estimated sedimentation. The age of the sediment in the lowermost part of the regular succession above igneous basement is lower Oligocene (between 32.02 and 32.20 Ma). This finding is in good agreement with the age of basement anticipated from regional magnetic surveys at 32.4 Ma.

5. Preliminary scientific assessment

The broad objective of Expedition 395 was to deliver the samples and data required to test a range of interdisciplinary scientific hypotheses about topics that include mantle convection and crustal accretion, paleoclimate, ocean circulation, and the deep limits of life. The expedition focused on a unique part of the North Atlantic Ocean where the Mid-Atlantic Ridge is strongly influenced by the Iceland mantle plume and where rapidly accumulated drift sediments record changes in deep-water circulation currents and climate on millennial timescales. Considered together, Expeditions 384, 395C and 395 were designed to target six primary sites with a combination of crustal and sedimentary sequences that were chosen to build on scientific breakthroughs from previous scientific drilling in the region, notably during DSDP Leg 49 and ODP Legs 105, 152, and 162.

Expedition 395 was the third of the three expeditions in the overall project, following Expedition 384 in 2020 (Blum et al., 2020), and Expedition 395C in 2021 (Parnell-Turner et al., 2022). Expedition 395 had three initial operational goals. First, to recover a complete sedimentary sequence for Gardar drift, followed by coring through 130 m of the underlying 32 My old basaltic crust (Site U1564). Second, to complete coring and sampling of the sedimentary succession of Björn drift at Sites U1554 and U1562, which were initially drilled during Expedition 395C, but without collecting a full stratigraphic splice and without a full set of ephemeral properties measurements. Third, time permitting, Expedition 395 aimed to recover a significant portion of the sedimentary section of Eirik drift on the eastern margin of Greenland (Site U1602), with a tentative objective of reaching late Miocene sediments near 7.8 Ma. As detailed below, all of these objectives were attained during Expedition 395, with the additional achievement of sampling extensive Paleogene and Neogene pre-drift sedimentary succession at Eirik drift (Site U1602) (Figure **F20**).

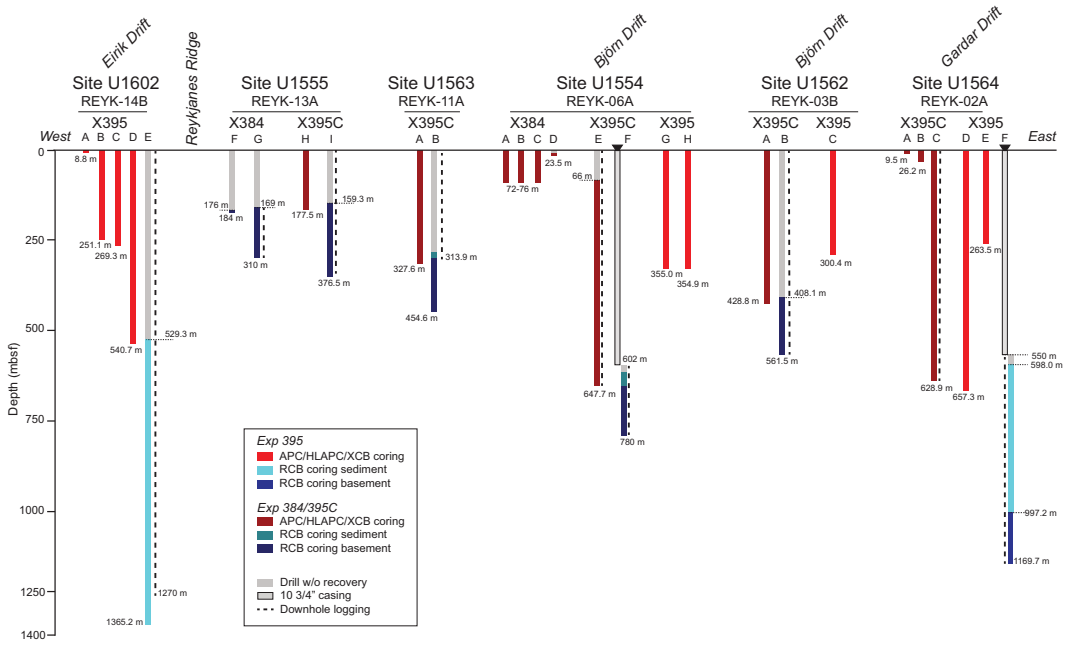

Figure F20. Summary of completed operations, Expeditions 384, 395C, and 395.

5.1. Operational achievements of Expedition 395

Each of the initial operational objectives of Expedition 395 were met, and in many cases exceeded. Initially planned to recover ~3500 m of core, Expedition 395 achieved a total penetration of 4429 m, recovering 3734.6 m of core with an overall recovery rate of 84% (Figure **F21**; Table **T1**). This total includes 66% recovery in the basalt section of Site U1564. The ephemeral properties measurements and microbiological sampling programs were remarkably successful during Expedition 395, collecting a total of 243 interstitial fluid samples to depths of up to 1050 m (achieved in Hole U1564F). The 33 microbiological samples collected from the basement section of Site U1564, at a spacing of ~5 m, represent one of the most complete records of their kind to date. The full planned suite of wireline logging data was collected at Site U1564, and although a stuck tool ended logging operations early, a partial wireline logging data set was still collected at Site U1602.

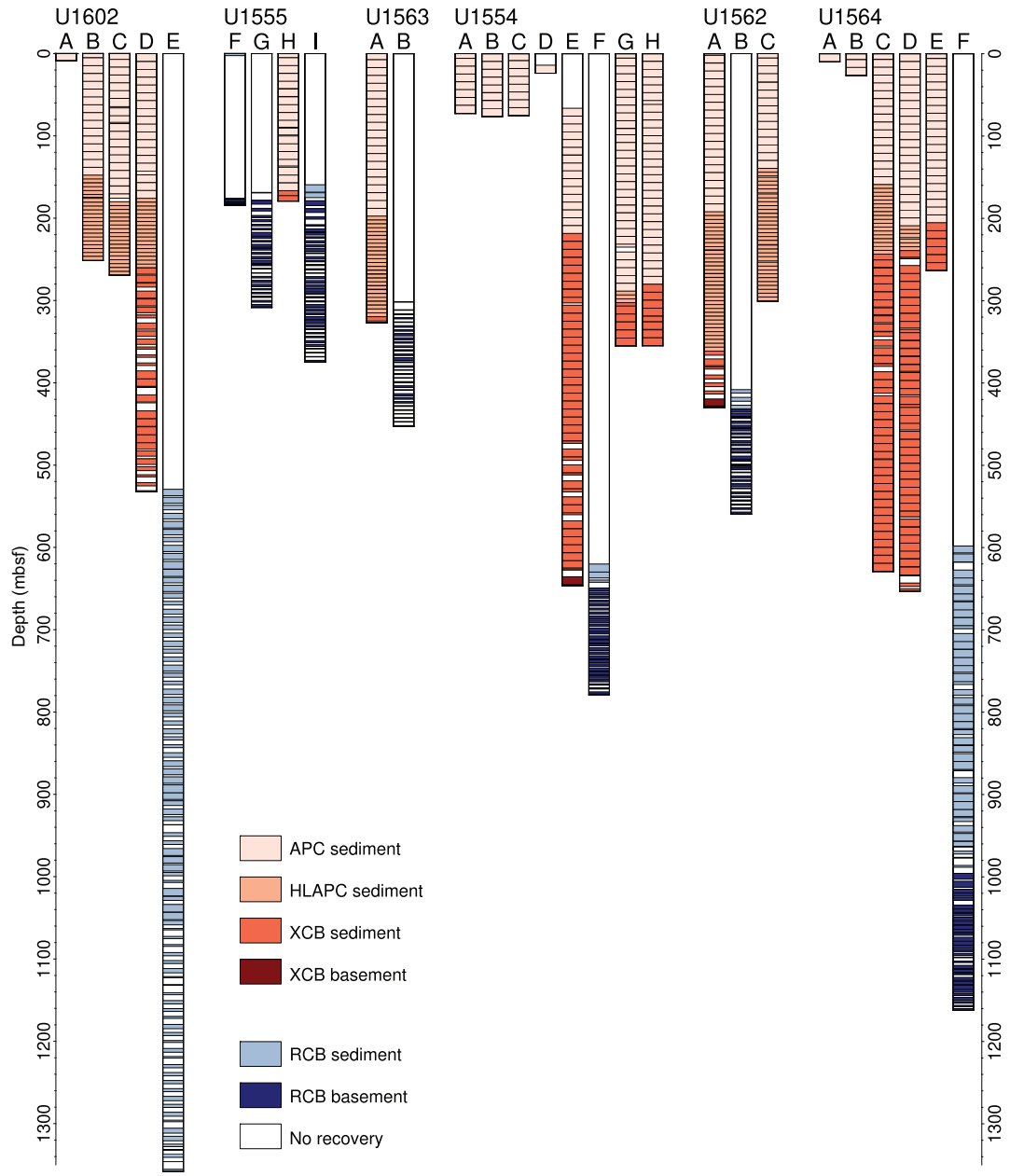

Figure F21. Core recovery summary, Expedition 395 project sites.

5.1.1. Objective 1: crustal accretion and V-shaped ridge origins

Basalt was drilled across the full planned interval at all five sites during Expeditions 384, 395C, and 395, fully satisfying the needs for crustal sampling of Objective 1. Material from segmented crust at Site U1564, potentially representing North Atlantic end-member crust not influenced by the Iceland plume, was cored during Expedition 395, and the other four sites, representing VSRs and VSTs, were drilled during Expeditions 384 and 395C. Expedition 395 succeeded in recovering 119 m of basaltic cores from the segmented, 32 My old oceanic crust which lies beneath Gardar drift at Site U1564. Combined with the basement material successfully recovered at VSR/VST pairs during Expeditions 384 and 395C, these basalts will enable the hypotheses for the origin of VSRs, and the dynamic behavior of the Iceland mantle plume to be tested. The large amount of basement material recovered from the five sites reveal variability in lava morphology (e.g., pillows versus sheet flows) between the sites, and preliminary shipboard geochemical analyses indicate differences in degrees of melting and/or variability in source composition. Postcruise geochemical measurements, lithologic analysis, and modeling will provide the foundations for evaluating existing hypotheses, in addition to furthering the exploration of crustal accretion processes along the plate spreading transect.

The high basement recovery rate helped meet the objective to sample a representative number of flow units from each site, minimizing possible sampling biases. Favorable weather and timing enabled deeper basalt penetration than originally planned at Sites U1555 and U1564. This additional recovery was particularly valuable at Site U1564, where a significant amount of glassy material was recovered toward the base of the hole, deeper than the initially planned 130 m basement penetration target. In the otherwise highly altered basaltic section at Site U1564, this glass will be invaluable for future geochemical analyses and will play a critical role in constraining mantle source composition and melting processes at the Reykjanes Ridge 32 My ago. The paired basement sections recovered in Holes 384-U1555G and 395C-U1555I represent a petrological splice through the basaltic basement, which leads to a rare opportunity to study both the spatial- and depth-dependent properties of the oceanic crust. The core recovery is paired with extensive downhole logging data sets, including FMS-sonic logs and UBI data, which provide a 360° view of the borehole. These images are of exceptional quality, providing insight into the eruptive units, structural features, and alteration character of the basalt sequence.

5.1.2. Objective 2: paleoclimate and deepwater circulation

To satisfy the needs of the paleoclimate and ocean circulation objectives, the first order operational aim of Expedition 395 was to collect near-complete splices through key sedimentary intervals of Gardar, Björn, and Eirik drifts. Enabled by the excellent work of the shipboard drilling and technical staff, complete splices throughout the APC-cored sections of each of these drifts were achieved. These splices include key climatic intervals such as the intensification of Northern Hemisphere Glaciation at 2.7 Ma, and the onset of contourite drift sedimentation. The shipboard data already reveal new insights into changes in sedimentation, climate and ocean circulation during these important intervals. Enabled by the high-sedimentation rate material recovered, postcruise analysis of Expedition 395 cores and data will be able to address detailed questions about climatic and oceanographic history of the North Atlantic region.

An important goal of Expedition 395 was to obtain high resolution records of sedimentation rate in contourite drift sediments across a North Atlantic transect at the key 60°N latitude. Expedition 395 sites were chosen to maximize the chance of success for this objective, located in undisturbed, rapidly deposited stratigraphy of Björn, Gardar and Eirik drifts. Continuous core recovery with near-continuous splices, well-resolved magnetostratigraphic records, and excellent microfossil preservation and biohorizons, means that the age models generated by Expedition 395 are exceptional in quality. These well-constrained models considerably extend previous reference models from ODP Sites 982 and 983, reaching from modern to Miocene (Björn drift), Oligocene (Gardar drift), and Eocene times (Eirik drift), and are important reference sections for the geologic history of the North Atlantic region. Importantly, Expedition 395 sites cored through the onset of sedimentation at major drifts in the North Atlantic Ocean, demonstrating the value of drilling sites with multiple holes across a transect.

Favorable weather and operational efficiencies meant that additional, initially unplanned APC coring was able to be carried out at Hole U1562C during Expedition 395. This site, located on the eastern fringe of Björn drift, contains a remarkably well preserved late Miocene record, owing to its relatively shallow burial depth. The additional APC hole enabled a continuous splice to be obtained through this key interval and is likely to yield important insights into this important climatic interval.

Operations during Expeditions 384 and 395C allowed the addition of Site U1602 to Expedition 395 (Parnell-Turner et al., 2023). Site U1602 recovered a unique record of sedimentation of Eirik drift back to the late Eocene, with implications for the stability of Greenland ice sheet and the evolution of the early North Atlantic Ocean by providing sedimentary records with standard pelagic microplankton groups preserved through large intervals, as well as the potential for biomarker proxy data generation. This record from Eirik drift is particularly valuable given ODP Site 646 only recovered a partial record of the drift and termination of the drilling program in 2024, which means that further drilling at Eirik drift likely will not be realized for decades to come.

Considered together, the excellent recovery and high-resolution magnetic recording potential of sediments across the transect of six sites will lead to a significant contribution to our understanding of Earth's magnetostratigraphic history. Although nearby ODP Sites 982 and 983 are reference sites for the fine-scale geomagnetic intensity timescale (GITS), the new material recovered from Expedition 395 will extend their records well beyond Quaternary times and beyond the Matuyama polarity chron. Comparison between the multiple high-resolution magnetostratigraphic records contained across Expedition 395 sites is likely to address existing uncertainty in the GITS, previously caused by reliance upon single sites.

The transect of Expedition 395 sites, spanning the central North Atlantic and proximal to the Greenland ice sheet, also is positioned to capture a continuous record of Pleistocene ice sheet dynamics. Combining the continuous recovery with novel shipboard X-ray images collected during Expedition 395 means that a detailed analysis of the pacing of IRD older than 1.8 Ma is likely possible. The recovery of laminated silt horizons on the Greenland margin at Site U1602 also opens the unexpected possibility to track ice sheet behavior through the record of meltwater pulses and grain provenance.

5.1.3. Objective 3: crustal aging and hydrothermal alteration

Altered basalt drilled at four sites up to 12.3 Ma in age during Expeditions 384 and 395C partially satisfied the needs for crustal sampling of Objective 3. However, the oldest crustal material, at Site U1564, was necessary to complete the 32 My transect as originally planned. The 119 m of basalt recovered during Expedition 395 at Site U1564 contains a rich variety of alteration fabrics, mineralogy, and structural features, that will enable the aims of Objective 3 to be satisfied. The successful acquisition of high-resolution 360° borehole images at all five basement sites, means that a full evaluation of the structural evolution of the basaltic crust will be feasible postcruise. Finally, the large number of microbiological samples collected across all sites will allow feedbacks between crustal alteration, fluid flow, and microbial life to be investigated in unprecedented detail.

The transect of sites east of the Reykjanes Ridge comprehensively sample the different controls at play in determining the extent and timing of crustal alteration. The unexpected deep sediment recovery from Site U1602, which comprises lithified sediment containing fractures with various mineral fill, allows new questions about the connectivity between crust, sediment, and ocean to be addressed.

The IW and microbial samples collected in both sediment and basalt during Expedition 395 form one of the most comprehensive collections of their kind ever obtained. Paired with a history of alteration recorded by exceptionally high recovery rates, the combined results of the six-site Expedition 395 project transect opens up new opportunities to explore the links between petrology, chemical exchange, alteration mineralogy, and microbial life within and between the basement, sediment and ocean.

The remarkable success of Expedition 395 was partly enabled by favorable weather conditions. More importantly, however, it was enabled by the well-established drilling and laboratory proce-

dures aboard *JOIDES Resolution*, which have been refined and perfected over decades of operation. Our success also relied upon the dedication and expertise of the shipboard drilling and technical staff, who bring with them decades of experience and knowledge. These technical, operational, and personnel resources will almost certainly be lost once *JOIDES Resolution* ceases to operate, at great cost to future generations of scientists.

6. Outreach

Expedition 395 had one onboard Outreach Officer, a secondary science teacher from Massachusetts, USA. The shipboard outreach program included posting to social media platforms, including X (formerly known as Twitter), Instagram, Facebook, and YouTube; creating blog posts; and communicating the science objectives during ship-to-shore broadcasts and for media inquiries. Finally, a classroom lesson focusing on biostratigraphy and glacial/interglacial periods was created with the help of one of the paleontologists and will be made available to the public.

6.1. Social media

Three main social media platforms were used to disseminate of the science objectives as well as information on the drilling process. 91 posts were made to Facebook. These garnered 231 Impressions, 3900 reactions with 149 comments, and 342 shares. While using the Facebook page, users clicked content links 570 times. Sixty-eight new followers were obtained on this platform. On Instagram, a mixture of reels and stories were posted for a total of 117 posts. These posts received 115,000 impressions, 93 comments/replies, and 5600 likes/reactions. There were 188 new followers added to the Instagram account during this time. 290 X (formerly known as Twitter) posts were recorded with 632,000 impressions, 181 comments, 8900 reactions, and 1500 shares. There were also 666 content link clicks on this platform. A total of 452 new X (formerly known as Twitter) followers were added to the @TheJR profile during this time.

A total of 13 blog posts were created, with topics including life on the JR, biostratigraphy, core curation, and drilling technology.

6.2. Ship-to-shore events

Twenty-five ship-to-shore events were held during Expedition 395. The Expedition 395 scientists assisted with these tours and on four occasions hosted the tours in their native languages. In addition to these events, there were two virtual Open Houses held. All of these events combined reached over 400,830 individuals from more than 15 different countries.

The events were primarily for college and graduate students, but all audiences were reached. One event was part of a lecture series for the PaleoPERCs program. Another event was part of a lunch session for a UK-IODP meeting. Summer camps and summer enrichment programs for middle school to high school students also attended these tours.

6.3. Media

One live broadcast interview was given by the Expedition Project Manager on Nebraska TV (NTV). The Outreach Officer aided in the creation of a media article for Marine Technology magazine and provided a Zoom tour for the journalist. Two articles for the monthly UK IODP magazine were written and published (July and August 2023 editions).

References

Bailey, I., Hole, G.M., Foster, G.L., Wilson, P.A., Storey, C.D., Trueman, C.N., and Raymo, M.E., 2013. An alternative suggestion for the Pliocene onset of major Northern Hemisphere glaciation based on the geochemical provenance of North Atlantic Ocean ice-rafted debris. Quaternary Science Reviews, 75:181–194. **https://doi.org/10.1016/j.quascirev.2013.06.004**

Barker, S., Chen, J., Gong, X., Jonkers, L., Knorr, G., and Thornalley, D., 2015. Icebergs not the trigger for North Atlantic cold events. Nature, 520(7547):333–336. **https://doi.org/10.1038/nature14330**

Barker, S., Knorr, G., Conn, S., Lordsmith, S., Newman, D., and Thornalley, D., 2019. Early interglacial legacy of deglacial climate instability. Paleoceanography and Paleoclimatology, 34(8):1455–1475. **https://doi.org/10.1029/2019PA003661**

Benediktsdóttir, Á., Hey, R., Martinez, F., and Höskuldsson, Á., 2012. Detailed tectonic evolution of the Reykjanes Ridge during the past 15 Ma. Geochemistry, Geophysics, Geosystems, 13(2):Q02008. **https://doi.org/10.1029/2011GC003948**

Blum, P., Rhinehart, B., and Acton, G.D., 2020. International Ocean Discovery Program Expedition 384 Preliminary Report. International Ocean Discovery Program. **https://doi.org/10.14379/iodp.pr.384.2020**

Bodine, J.H., Steckler, M.S., and Watts, A.B., 1981. Observations of flexure and the rheology of the oceanic lithosphere. Journal of Geophysical Research: Solid Earth, 86(B5):3695–3707. **https://doi.org/10.1029/JB086iB05p03695**

Bond, G., Broecker, W., Johnsen, S., McManus, J., Labeyrie, L., Jouzel, J., and Bonani, G., 1993. Correlations between climate records from North Atlantic sediments and Greenland ice. Nature, 365(6442):143–147. **https://doi.org/10.1038/365143a0**

Briais, A., and Rabinowicz, M., 2002. Temporal variations of the segmentation of slow to intermediate spreading mid-ocean ridges, 1. Synoptic observations based on satellite altimetry data. Journal of Geophysical Research: Solid Earth, 107(B5):2098. **https://doi.org/10.1029/2001JB000533**

Channell, J.E.T., Mazaud, A., Sullivan, P., Turner, S., and Raymo, M.E., 2002. Geomagnetic excursions and paleointensities in the Matuyama Chron at Ocean Drilling Program Sites 983 and 984 (Iceland Basin). Journal of Geophysical Research: Solid Earth, 107(B6):2114. **https://doi.org/10.1029/2001JB000491**

Coggon, R.M., and Teagle, D.A.H., 2011. Hydrothermal calcium-carbonate veins reveal past ocean chemistry. TrAC Trends in Analytical Chemistry, 30(8):1252–1268. **https://doi.org/10.1016/j.trac.2011.02.011**

Dupré, B., and Allègre, C.J., 1980. Pb–Sr–Nd isotopic correlation and the chemistry of the North Atlantic mantle. Nature, 286(5768):17–22. **https://doi.org/10.1038/286017a0**

Fitton, J.G., Saunders, A.D., Norry, M.J., Hardarson, B.S., and Taylor, R.N., 1997. Thermal and chemical structure of the Iceland Plume. Earth and Planetary Science Letters, 153(3–4):197–208. **https://doi.org/10.1016/S0012-821X(97)00170-2**

Gillis, K.M., and Coogan, L.A., 2011. Secular variation in carbon uptake into the ocean crust. Earth and Planetary Science Letters, 302(3–4):385–392. **https://doi.org/10.1016/j.epsl.2010.12.030**

Hart, S.R., Schilling, J.G., and Powell, J.L., 1973. Basalts from Iceland and along the Reykjanes Ridge: Sr isotope geochemistry. Nature Physical Science, 246(155):104–107. **https://doi.org/10.1038/physci246104a0**

Hartley, R.A., Roberts, G.G., White, N., and Richardson, C., 2011. Transient convective uplift of an ancient buried landscape. Nature Geoscience, 4(8):562–565. **https://doi.org/10.1038/ngeo1191**

Hey, R., Martinez, F., Höskuldsson, Á., and Benediktsdóttir, Á., 2010. Propagating rift model for the V-shaped ridges south of Iceland. Geochemistry, Geophysics, Geosystems, 11(3):Q03011. **https://doi.org/10.1029/2009GC002865**

Jansen, E., and Raymo, M.E., 1996. Leg 162: new frontiers on past climates. In Jansen, E., Raymo, M.E., Blum, P., et al., Proceedings of the Ocean Drilling Program, Initial Reports. 162: College Station, TX (Ocean Drilling Program), 5–20. **https://doi.org/10.2973/odp.proc.ir.162.101.1996**

Jones, S.M., Murton, B.J., Fitton, J.G., White, N.J., Maclennan, J., and Walters, R.L., 2014. A joint geochemical–geophysical record of time-dependent mantle convection south of Iceland. Earth and Planetary Science Letters, 386:86–97. **https://doi.org/10.1016/j.epsl.2013.09.029**

Jones, S.M., White, N., and Maclennan, J., 2002. V-shaped ridges around Iceland: implications for spatial and temporal patterns of mantle convection. Geochemistry, Geophysics, Geosystems, 3(10):1–23. **https://doi.org/10.1029/2002GC000361**

Kempton, P.D., Fitton, J.G., Saunders, A.D., Nowell, G.M., Taylor, R.N., Hardarson, B.S., and Pearson, G., 2000. The Iceland plume in space and time: a Sr–Nd–Pb–Hf study of the North Atlantic rifted margin. Earth and Planetary Science Letters, 177(3):255–271. **https://doi.org/10.1016/S0012-821X(00)00047-9**

Kleiven, H.F., Hall, I.R., McCave, I.N., Knorr, G., and Jansen, E., 2011. Coupled deep-water flow and climate variability in the middle Pleistocene North Atlantic. Geology, 39(4):343–346. **https://doi.org/10.1130/G31651.1**

Krause, D.C., and Schilling, J.-G., 1969. Dredged basalt from the Reykjanes Ridge, North Atlantic. Nature, 224(5221):791–793. **https://doi.org/10.1038/224791b0**

Le Voyer, M., Kelley, K.A., Cottrell, E., and Hauri, E.H., 2017. Heterogeneity in mantle carbon content from CO_2-undersaturated basalts. Nature Communications, 8(1):14062. **https://doi.org/10.1038/ncomms14062**

Luyendyk, B.P., Cann, J.R., Duffield, W.A., Faller, A.M., Kobayashi, K., Poore, R.Z., Roberts, W.P., Sharman, G., Shor, A.N., Steiner, M., Steinmetz, J.C., Varet, J., Vennum, W., Wood, D.A., and Zolotarev, B.P., 1979. Initial Reports of the Deep Sea Drilling Project: Ocean Drilling Program, College Station, TX, United States (Texas A & M University). **http://hdl.handle.net/10.2973/dsdp.proc.49.1979**

Martinez, F., Hey, R., and Höskuldsson, Á., 2020. Reykjanes Ridge evolution: effects of plate kinematics, small-scale upper mantle convection and a regional mantle gradient. Earth-Science Reviews, 206:102956. **https://doi.org/10.1016/j.earscirev.2019.102956**

Martinez, F., and Hey, R., 2017. Propagating buoyant mantle upwelling on the Reykjanes Ridge. Earth and Planetary Science Letters, 457:10–22. **https://doi.org/10.1016/j.epsl.2016.09.057**

McCave, I.N., Thornalley, D.J.R., and Hall, I.R., 2017. Relation of sortable silt grain-size to deep-sea current speeds: calibration of the 'Mud Current Meter'. Deep Sea Research, Part I: Oceanographic Research Papers, 127:1–12. **https://doi.org/10.1016/j.dsr.2017.07.003**

Menviel, L., Timmermann, A., Friedrich, T., and England, M.H., 2014. Hindcasting the continuum of Dansgaard–Oeschger variability: mechanisms, patterns and timing. Climate of the Past, 10(1):63–77. **https://doi.org/10.5194/cp-10-63-2014**

Murton, B.J., Taylor, R.N., and Thirlwall, M.F., 2002. Plume–ridge Interaction: a geochemical perspective from the Reykjanes Ridge. Journal of Petrology, 43(11):1987–2012. **https://doi.org/10.1093/petrology/43.11.1987**

Parnell-Turner, R., Briais, A., and LeVay, L.J., 2022. Expedition 395C Preliminary Report: Reykjanes Mantle Convection and Climate: Crustal Objectives. International Ocean Discovery Program. **https://doi.org/10.14379/iodp.pr.395C.2022**

Parnell-Turner, R., Briais, A., and LeVay, L.J., 2023. Expedition 395 Scientific Prospectus Addendum: Reykjanes Mantle Convection and Climate. International Ocean Discovery Program. **https://doi.org/10.14379/iodp.sp.395add.2023**

Parnell-Turner, R., White, N., Henstock, T., Murton, B., Maclennan, J., and Jones, S.M., 2014. A continuous 55-million-year record of transient mantle plume activity beneath Iceland. Nature Geoscience, 7(12):914–919. **https://doi.org/10.1038/ngeo2281**

Parnell-Turner, R., White, N., Henstock, T.J., Jones, S.M., Maclennan, J., and Murton, B.J., 2017. Causes and consequences of diachronous v-shaped ridges in the North Atlantic Ocean. Journal of Geophysical Research: Solid Earth, 122(11):8675–8708. **https://doi.org/10.1002/2017JB014225**

Parnell-Turner, R., White, N.J., McCave, I.N., Henstock, T.J., Murton, B., and Jones, S.M., 2015. Architecture of North Atlantic contourite drifts modified by transient circulation of the Icelandic mantle plume. Geochemistry, Geophysics, Geosystems, 16(10):3414–3435. **https://doi.org/10.1002/2015GC005947**

Parnell-Turner, R.E., White, N.J., Maclennan, J., Henstock, T.J., Murton, B.J., and Jones, S.M., 2013. Crustal manifestations of a hot transient pulse at 60°N beneath the Mid-Atlantic Ridge. Earth and Planetary Science Letters, 363:109–120. **https://doi.org/10.1016/j.epsl.2012.12.030**

Poore, H., White, N., and Maclennan, J., 2011. Ocean circulation and mantle melting controlled by radial flow of hot pulses in the Iceland plume. Nature Geoscience, 4(8):558–561. **https://doi.org/10.1038/ngeo1161**

Poore, H.R., Samworth, R., White, N.J., Jones, S.M., and McCave, I.N., 2006. Neogene overflow of northern component water at the Greenland-Scotland Ridge. Geochemistry, Geophysics, Geosystems, 7(6):Q06010. **https://doi.org/10.1029/2005GC001085**

Rabinowicz, M., and Briais, A., 2002. Temporal variations of the segmentation of slow to intermediate spreading mid-ocean ridges, 2. A three-dimensional model in terms of lithosphere accretion and convection within the partially molten mantle beneath the ridge axis. Journal of Geophysical Research: Solid Earth, 107(B6):2110. **https://doi.org/10.1029/2001JB000343**

Raymo, M.E., Ganley, K., Carter, S., Oppo, D.W., and McManus, J., 1998. Millennial-scale climate instability during the early Pleistocene epoch. Nature, 392(6677):699–702. **https://doi.org/10.1038/33658**

Rickers, F., Fichtner, A., and Trampert, J., 2013. The Iceland–Jan Mayen plume system and its impact on mantle dynamics in the North Atlantic region: evidence from full-waveform inversion. Earth and Planetary Science Letters, 367:39–51. **https://doi.org/10.1016/j.epsl.2013.02.022**

Schilling, J.G., 1973. Iceland mantle plume: geochemical study of Reykjanes Ridge. Nature, 242(5400):565–571. **https://doi.org/10.1038/242565a0**

Schoonman, C.M., White, N.J., and Pritchard, D., 2017. Radial viscous fingering of hot asthenosphere within the Icelandic plume beneath the North Atlantic Ocean. Earth and Planetary Science Letters, 468:51–61. **https://doi.org/10.1016/j.epsl.2017.03.036**

Sclater, J.G., Jaupart, C., and Galson, D., 1980. The heat flow through oceanic and continental crust and the heat loss of the Earth. Reviews of Geophysics, 18(1):269-311. **https://doi.org/10.1029/RG018i001p00269**

Shorttle, O., and Maclennan, J., 2011. Compositional trends of Icelandic basalts: implications for short–length scale lithological heterogeneity in mantle plumes. Geochemistry, Geophysics, Geosystems, 12(11):Q11008. **https://doi.org/10.1029/2011GC003748**

Thornalley, D.J.R., Blaschek, M., Davies, F.J., Praetorius, S., Oppo, D.W., McManus, J.F., Hall, I.R., Kleiven, H., Renssen, H., and McCave, I.N., 2013. Long-term variations in Iceland–Scotland overflow strength during the Holocene. Climate of the Past, 9(5):2073–2084. **https://doi.org/10.5194/cp-9-2073-2013**

Vogt, P.R., 1971. Asthenosphere motion recorded by the ocean floor south of Iceland. Earth and Planetary Science Letters, 13(1):153–160. **https://doi.org/10.1016/0012-821X(71)90118-X**

White, R.S., 1997. Rift–plume interaction in the North Atlantic. Philosophical Transactions of the Royal Society, A: Mathematical, Physical and Engineering Sciences, 355(1723):319–339. **https://doi.org/10.1098/rsta.1997.0011**

White, R.S., Bown, J.W., and Smallwood, J.R., 1995. The temperature of the Iceland plume and origin of outward-propagating V-shaped ridges. Journal of the Geological Society (London, UK), 152(6):1039–1045. **https://doi.org/10.1144/GSL.JGS.1995.152.01.26**

Wood, D.A., Tarney, J., Varet, J., Saunders, A.D., Bougault, H., Joron, J.L., Treuil, M., and Cann, J.R., 1979. Geochemistry of basalts drilled in the North Atlantic by IPOD Leg 49: implications for mantle heterogeneity. Earth and Planetary Science Letters, 42(1):77–97. **https://doi.org/10.1016/0012-821X(79)90192-4**

Wright, J.D., and Miller, K.G., 1996. Control of North Atlantic Deep Water circulation by the Greenland-Scotland Ridge. Paleoceanography and Paleoclimatology, 11(2):157–170. **https://doi.org/10.1029/95PA03696**